

## UNVEILING THE NATURE OF THE UNIDENTIFIED $\gamma$ -RAY SOURCES I: A NEW METHOD FOR THE ASSOCIATION OF $\gamma$ -RAY BLAZARS

R. D'ABRUSCO<sup>1</sup>, F. MASSARO<sup>2</sup>, A. PAGGI<sup>1</sup>, N. MASETTI<sup>3</sup>, G. TOSTI<sup>4,5</sup>, M. GIROLETTI<sup>6</sup> & H. A. SMITH<sup>1</sup>.

version January 27, 2020: fm

### ABSTRACT

We present a new method for identifying blazar candidates by examining the *locus*, i.e. the region occupied by the *Fermi*  $\gamma$ -ray blazars in the three-dimensional color space defined by the *WISE* infrared colors. This method is a refinement of our previous approach that made use of the two-dimensional projection of the distribution of *WISE*  $\gamma$ -ray emitting blazars (the *Strip*) in the three *WISE* color-color planes Massaro et al. (2012a). In this paper, we define the three-dimensional *locus* by means of a Principal Component (PCs) analysis of the colors distribution of a large sample of blazars composed by all the ROMA-BZCAT sources with counterparts in the *WISE* All-Sky Catalog and associated to  $\gamma$ -ray source in the second *Fermi* LAT catalog (2FGL) (the *WISE Fermi* Blazars sample, WFB). Our new procedure yields a total completeness of  $c_{\text{tot}} \sim 81\%$  and total efficiency of  $e_{\text{tot}} \sim 97\%$ . We also obtain local estimates of the efficiency and completeness as functions of the *WISE* colors and galactic coordinates of the candidate blazars. The catalog of all *WISE* candidate blazars associated to the WFB sample is also presented, complemented by archival multi-frequency information for the alternative associations. Finally, we apply the new association procedure to all  $\gamma$ -ray blazars in the 2FGL and provide a catalog containing all the  $\gamma$ -ray candidates blazars selected according to our procedure.

*Subject headings:* galaxies: active - galaxies: BL Lacertae objects - radiation mechanisms: non-thermal

### 1. INTRODUCTION

Unveiling the nature of the Unidentified Gamma-ray Sources (UGS) is one of the main scientific objectives of the ongoing *Fermi*  $\gamma$ -ray mission. Recently, several attempts have been performed to associate or characterize the UGSs, either using X-ray observations (e.g., Mirabal 2009; Mirabal & Halpern 2009) or with statistical approaches (e.g. Mirabal et al. 2010; Ackermann et al. 2012). Nevertheless, according to Nolan et al. (2012), 31% of the  $\gamma$ -ray sources in the second *Fermi* LAT catalog (2FGL) remain unidentified and many of these unidentified sources could be blazars, since blazars are known to dominate the  $\gamma$ -ray sky (e.g. Hartman et al. 1999; Abdo et al. 2010a), and among the 1297 associated sources within the 2FGL, 805 (62%) are known blazars Nolan et al. (2012). Therefore it is important to devise an efficient means of identifying candidate blazars among these sources.

Blazars are radio-loud Active Galactic Nuclei (AGNs) characterized by high and variable polarization, apparent superluminal motions, and high luminosities (e.g., Urry & Padovani 1995). They exhibit a flat radio spectrum that steepens toward the infrared-optical bands. They also show rapid variability from the radio to  $\gamma$ -rays

and have peculiar infrared colors (Massaro et al. 2011a). Their characteristic spectral energy distributions (SEDs) have two main components: the low-energy component peaking in the spectral range from the IR to the X-ray band and the high-energy component peaking from MeV to TeV energies.

Blazars come in two main classes: the BL Lac objects, which have featureless optical spectra, and the more luminous Flat-Spectrum Radio Quasars which, typically, show prominent optical spectral emission lines (Stickel et al. 1991; Stoke et al. 1991). In the following discussion, we label the BL Lac objects as BZBs and the Flat-Spectrum Radio Quasars as BZQs, following the nomenclature of the Multi-wavelength Catalog of blazars (ROMA-BZCAT, Massaro et al. 2009).

Data from *WISE* have been recently used to select and classify AGNs (Stern et al. 2012; Yan et al. 2013) from a general point of view. The specific problem of the classification and identification of  $\gamma$ -ray sources has been tackled using machine learning techniques (Hassan et al. 2013) and characterizing their optical variability (Ruan et al. 2012). Additional attempts to find counterparts of UGSs have been carried out using radio follow up observations (e.g., Kovalev et al. 2009; Kovalev 2009).

Using the preliminary data release of the Wide-field Infrared Survey Explorer (*WISE*) (see Wright et al. 2010, for more details)<sup>7</sup>, we showed that the  $\gamma$ -ray blazar population occupies a distinctive region of the *WISE* color parameter space (called the *WISE* Gamma-ray *Strip* Massaro et al. (2011a); D'Abrusco et al. (2012); hereinafter, Papers I and II respectively).

We then used the results of our analyses to develop a new association method to investigate the nature of the

<sup>1</sup> Harvard - Smithsonian Astrophysical Observatory, 60 Garden Street, Cambridge, MA 02138, USA

<sup>2</sup> SLAC National Laboratory and Kavli Institute for Particle Astrophysics and Cosmology, 2575 Sand Hill Road, Menlo Park, CA 94025, USA

<sup>3</sup> INAF/IASF di Bologna, via Gobetti 101, I-4019 Bologna, Italy

<sup>4</sup> Dipartimento di Fisica, Università degli Studi di Perugia, 06123 Perugia, Italy

<sup>5</sup> Istituto Nazionale di Fisica Nucleare, Sezione di Perugia, 06123 Perugia, Italy

<sup>6</sup> INAF Istituto di Radioastronomia, via Gobetti 101, 40129, Bologna, Italy

<sup>7</sup> <http://wise2.ipac.caltech.edu/docs/release/prelim/>

unidentified  $\gamma$ -ray sources in the 2FGL (Massaro et al. 2012a,b, Paper III and IV) as well as the unidentified *INTEGRAL* sources (Massaro et al. 2012c, Paper V). Adopting our new association procedure, we have succeeded in finding low-energy counterpart candidates for 156 out of 313 ( $\sim 50\%$ ) of the unidentified  $\gamma$ -ray sources analyzed (Paper IV).

Taking advantage of the much larger data set now available thanks to the *WISE* All-Sky archive<sup>8</sup>, released in March 2012, in this work we present a revisited definition of the region occupied by the  $\gamma$ -ray blazars. We will refer to the 3-dimensional region occupied by the  $\gamma$ -ray emitting blazars as the *locus* while we will continue to indicate the 2-dimensional projection of the *locus* in the  $[3.4] - [4.6]$  vs  $[4.6] - [12]$   $\mu\text{m}$  color-color plane as *WISE* Gamma-ray *Strip*. In this paper we determine a geometrical description of the WFB *locus* in the space generated by the Principal Components of their distribution in the *WISE* color space and apply our association procedure the whole sample of blazars that belong to the 2FGL.

The paper is organized as follows: in Section 2 we describe the selection criteria adopted to create the samples needed for our investigation, together with the method for the positional associations between the ROMA-BZCAT and the *WISE* archive. In Section 3 we describe the new geometric model of the WFB *locus* in the PCs space and define the quantitative parameter used to measure the compatibility of a generic *WISE* source with the *locus*. Section 4 is devoted to the association procedure based on the new parametrization of the *locus*. In Section 5 and Section 7 we describe the results of the application of the new association procedure to the WFB sample (with the estimates of the completeness and efficiency of the process) and to the sample of 2FGL *Fermi* blazars, respectively. Section 6 discusses the evaluation of the efficiency and completeness of the association procedure based on the results of the re-association of the WFB sample presented in Section 5. In Section 8 we summarize the results of this paper and draw some conclusions.

The *WISE* magnitudes in the  $[3.4]$ ,  $[4.6]$ ,  $[12]$ ,  $[22]$   $\mu\text{m}$  nominal *WISE* filters are in the Vega system. We indicate the *WISE* colors  $[3.4]-[4.6]$ ,  $[4.6]-[12]$  and  $[12]-[22]$  as  $c_1$ ,  $c_2$  and  $c_3$  and their corresponding errors as  $\sigma_{c_1}$ ,  $\sigma_{c_2}$  and  $\sigma_{c_3}$ , respectively. The values of the first two *WISE* magnitudes, namely  $[3.4]$  and  $[4.6]$  and, in turn, of the two derived colors  $c_1$  and  $c_2$ , have been corrected for galactic extinction according to the extinction law presented in Draine (2003). The corrections on the remaining two *WISE* magnitudes ( $[12]$  and  $[22]$ ) are negligible. All color values in the paper are corrected for galactic extinction. All the acronyms used in the paper are listed in Table 1.

## 2. THE SAMPLE SELECTION

### 2.1. The ROMA-BZCAT

The starting sample used in our analysis is the one presented in the ROMA-BZCAT v4.1, released in August 2012, the most comprehensive blazars catalog existing in literature with 3149 *bona fide* blazars and blazar candidates. The catalog includes 1220 BZBs, divided as

<sup>8</sup> <http://wise2.ipac.caltech.edu/docs/release/allsky/>

**Table 1**  
List of acronyms and specific terms used in this paper.

Name	Acronym
Multiwavelength Catalog of blazars	ROMA-BZCAT
Second <i>Fermi</i> Large Area Telescope catalog	2FGL
Second <i>Fermi</i> LAT Catalog of AGNs	2LAC
BL Lac object	BZB
Flat Spectrum Radio Quasar	BZQ
Blazar of Uncertain type	BZU
<i>WISE Fermi</i> Blazars sample	WFB
2D region of the $c_2$ vs $c_1$ color-color plane occupied by the WFB sample	<i>strip</i>
3D region of the <i>WISE</i> color space occupied by the WFB sample	<i>locus</i>
<i>Fermi</i> 2FGL Blazars sample	2FB
Search Region for candidate blazars	SR
Background Region for candidate blazars	BR
Principal Components	PCs

950 BL Lacs, 270 BL Lac candidates, 1707 BZQs and 222 blazars of Uncertain type (BZUs) (Massaro et al. 2011a). All the details about the ROMA-BZCAT catalog and the surveys used to build it can be found in (Massaro et al. 2009, 2010, 2011b)<sup>9</sup>.

### 2.2. ROMA-BZCAT to *WISE* positional associations

We remark that the coordinates reported in the ROMA-BZCAT are non-uniform. The astrometric accuracy can be as low as  $\sim 5''$ , corresponding to the uncertainty of the NRAO Very Large Array Sky Survey (NVSS) for sources with radio fluxes close to the survey limit (Condon et al. 1998). For this reason, we have developed a method to perform the positional association between the ROMA-BZCAT blazars and their *WISE* counterparts. All *WISE* sources considered in our analysis are detected in at least one *WISE* band with a signal-to-noise ratio (SNR) higher than 5 in the *WISE* All-Sky .

For each blazar, we searched for IR counterparts of the ROMA-BZCAT blazars in the *WISE* all-sky archive within circular regions of variable radius  $R$  in the range between  $0''$  and  $6.5''$ . For each value of  $R$ , we estimated the number of total  $N_t(R)$  and random matches  $N_r(R)$ , respectively, together with the chance probability for the spurious associations,  $p(R)$  calculated as follows. The random matches  $N_r(R)$  correspond to those found shifting the blazar coordinates by a fixed distance of  $20''$  in a random direction of the sky. This distance of  $20''$  has been chosen because it is larger than the maximum positional uncertainty on the coordinates reported in the ROMA-BZCAT. The chance probability for spurious associations  $p(R)$  is calculated as the ratio between  $N_r(R)$  and the total number of blazars listed in the ROMA-BZCAT (i.e., 3149).

Then, we calculated the differences between the number of associations at given radius  $R$  and those at  $R - \Delta R$  for total matches, defined as:

$$\Delta N_t(R) = N_t(R) - N_t(R - \Delta R) , \quad (1)$$

and the corresponding variation of the random associations,  $\Delta N_r(R)$ :

$$\Delta N_r(R) = N_r(R) - N_r(R - \Delta R) , \quad (2)$$

<sup>9</sup> <http://www.asdc.asi.it/bzcat/>

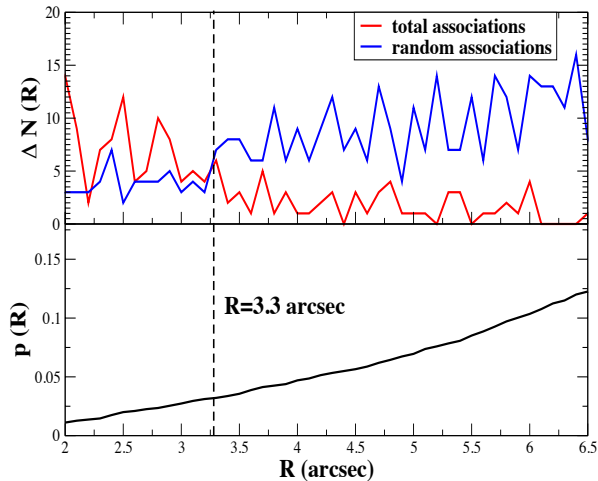


**Figure 1.** Upper panel) The number of total  $N_t(R)$  (red line) and random matches  $N_r(R)$  (blue line) as function of the radius  $R$  between  $2''$  and  $6.5''$ , respectively. The radial threshold selected for our ROMA-BZCAT - *WISE* crossmatches is indicated by the vertical dashed black line (see Section 2 for more details). Lower panel) The chance probability for the spurious associations,  $p(R)$  as function of the radius  $R$  between  $2''$  and  $6.5''$ .

where  $\Delta R = 0.1''$ .

Figure 1 shows the curves corresponding to  $\Delta N_t(R)$ ,  $\Delta N_r(R)$  and  $p(R)$  for different values of the radius  $R$  between  $2''$  and  $6.5''$ . For all radii larger than  $3.3''$  we found that the increase in number of IR sources positionally associated with blazars in the ROMA-BZCAT becomes systematically lower than the increase in number of random associations; thus we chose this value as our radial threshold in searching for counterparts of ROMA-BZCAT blazars in the *WISE* all-sky release. A similar positional association method has been adopted for the *INTEGRAL* sources (Stephen et al. 2006), while the chance probability for the spurious associations,  $p(R)$  has been estimated according to the procedure used for the *SWIFT* blazars detected in the hard X-rays by the BAT instrument on board (Maselli et al. 2010a,b). We followed the same recipe also for searching the *WISE* blazars counterparts in Paper I.

### 2.3. The *WISE* Fermi Blazars sample

We found 3032 out of 3149 (i.e., 96.3% of the ROMA-BZCAT) blazars with an IR counterpart within  $3.3''$  in the *WISE* All-Sky data archive. In this sample, there are only 2 multiple matches out of 3032 spatial associations, for which we used the IR data of the closest *WISE* source in the following analysis. The probability of a chance associations for these 3032 is  $\sim 3.3\%$  (see Figure 1), implying that  $\sim 100$  sources associated within the above radius could be spurious associations.

Of these 3032 blazars, 1172 are BZBs, including 919 BL Lacs and 253 BL Lac candidates, 1642 are BZQs and 218 are BZUs. It is also worth noticing that all the blazars associated between the ROMA-BZCAT and the *WISE* all-sky data release are detected in the first two filters at  $3.4$  and  $4.6 \mu\text{m}$ . We also checked the properties of the blazars that have not been associated or do not have a

counterpart in the *WISE* all-sky catalog, and we found that they do not appear to have peculiar properties in the radio, optical or X-ray energy range on the basis of the data reported in the ROMA-BZCAT.

Among the 3032 selected blazars, only 673 have a counterpart in the  $\gamma$ -rays according to the 2FGL and to the CLEAN sample presented in the second *Fermi* LAT Catalog of active galactic nuclei (2LAC; Ackermann et al. 2011). 637/673 (i.e., 94.7%) of these blazars (333 BZBs, 277 BZQs, and 27 BZUs) are detected in all four *WISE* bands. As in Paper III the sample of  $\gamma$ -ray emitting blazars in the ROMA-BZCAT catalog was derived excluding the BZUs sources from our sample of  $\gamma$ -ray loud blazars. For this reason, the final WFB sample includes only 610 *WISE* sources out of 673 *WISE* counterparts.

### 3. THE *LOCUS* PARAMETRIZATION

In paper III we characterized the region occupied by the  $\gamma$ -ray blazars in the *WISE* IR color space by considering the three different two-dimensional projections in the color-color planes built with the *WISE* filters separately. Taking advantage of the *WISE* All-Sky archive recently released, in this paper we refine our previous definition of the *locus* and improve significantly our association procedure by modeling the *locus* occupied by the  $\gamma$ -ray blazars directly in the three dimensional parameter space generated by the four *WISE* filters. This new parametrization and the improved association procedure replace our previous analyses.

#### 3.1. The locus in the Principal Components space

The new parametrization of the WFB *locus* is based on a new model of the *locus* in the PCs space generated by the *WISE* colors of the WFB *WISE* counterparts, and on a more versatile definition of the statistical quantity used to evaluate the compatibility of a generic *WISE* source with the *locus* model, the score. The distribution of the WFB sources in the three-dimensional *WISE* color space is axisymmetric along a slew line (see Figure 2), so that a simple geometrical description of the *locus* can be determined in the PCs space.

Principal Component Analysis (PCA) uses an orthogonal transformation to convert a set of observations of possibly correlated variables into a set of values of linearly uncorrelated variables, the PCs. This transformation  $T: (c_1, c_2, c_3) \rightarrow (\text{PC}_1, \text{PC}_2, \text{PC}_3)$  is defined so that the first PC ( $\text{PC}_1$ ) accounts for as much of the variance in the data as possible, and each following component ( $\text{PC}_2$ ,  $\text{PC}_3$ , etc. up to the dimensionality of the initial space) has the highest variance possible under the constraint that it is orthogonal to the preceding components. In our case, the WFB sources in the three-dimensional PCs space based on their color distributions lie almost perfectly along the  $\text{PC}_1$  axis and are distributed symmetrically in the  $\text{PC}_2$  vs  $\text{PC}_3$  plane around the  $\text{PC}_1$  line. Based on the shape of the *locus* in the PCs space, we choose to define its geometrical model using a cylindrical parametrization, with axis aligned along the  $\text{PC}_1$  axis. The *locus*, as a whole, is modeled by three distinct cylinders: the first two of these cylindrical regions are dominated by BZB and BZQ sources respectively, while the third cylinder is defined as the region where the WFB population is *mixed* in terms of spectral classes (the Mixed region, hereinafter).

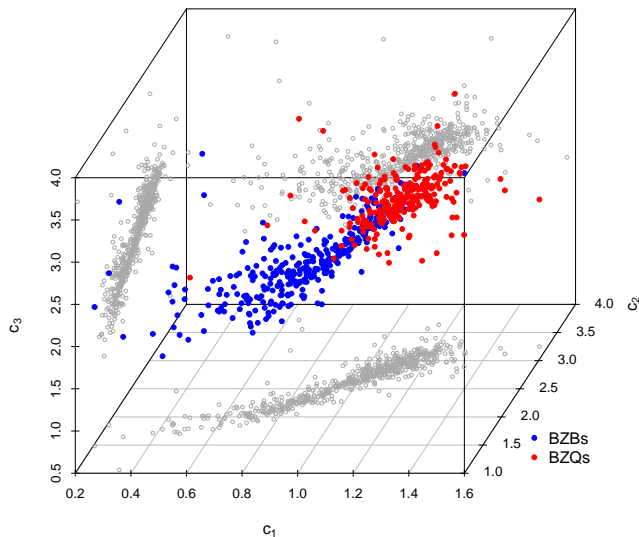


**Figure 2.** Scatterplot of the WFB sources in the three-dimensional *WISE* color space. The spectral class of the WFB sources is color-coded, while the three distributions of gray points represent the projections of the WFB sample in the three-dimensional color space onto the three two-dimensional color planes generated by the *WISE* colors  $c_1$ ,  $c_2$  and  $c_3$  respectively.

The upper and lower boundaries of the model along the  $PC_1$  axis have been determined requiring that 90% of the total number of WFB sources is contained within the boundaries of the cylinder, with 5% of the sources outside of the boundaries of the model on each side of the model along the  $PC_1$  axis. The boundaries of the Mixed section along the  $PC_1$  axis have been defined by requiring that, in this region, the fraction of either spectral class is smaller than 80% of the total number of WFB sources. The three boundaries along the  $PC_1$  axis defining the three sections of the WFB *locus* model are shown in Figure. 3.

The variances of the distribution of the WFB distribution in the PC space along the second and third PCs are  $\sigma_{PC_2}^2 = 0.61$  and  $\sigma_{PC_3}^2 = 0.58$  respectively. Based on this fact, we have modeled the bases of the cylinders as circles centered on the axis of the first principal component  $PC_1$  (the variance of the WFB distribution along  $PC_1$  is  $\sigma_{PC_3}^2 = 1.53$ ). The radii of the circular bases of each of the three cylinders representing the three different sections of the WFB *locus* in the PCs space have been determined independently as the radii containing the 90% of the WFB sources in each section. The radii of each of the three cylinders are defined in the plane generated by the  $PC_2$  and  $PC_3$  axes and evaluate  $d$  as  $R = \sqrt{PC_2^2 + PC_3^2}$ . The cumulative radial profiles of the three sections and the corresponding radii determined as discussed above are shown in Figure 4. The numerical values of the boundaries along the  $PC_1$  axis and the radii of the three cylinders of the new model of the WFB *locus* are reported in Table 2.

### 3.2. The score

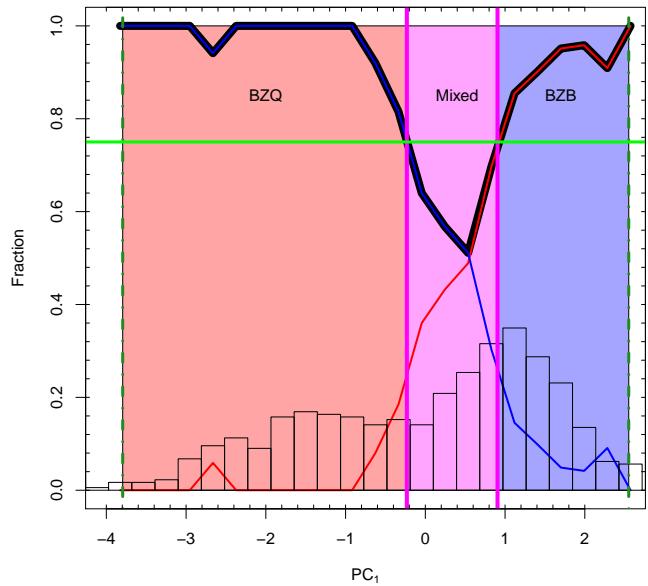


**Figure 3.** Boundaries of the three sections of the WFB *locus* in the PCs space along the  $PC_1$  axis. The solid black line represent the “purity” of the WFB population, i.e. the fraction of the dominant spectral class relative to the other spectral class. The solid red and blue lines represent the fraction of BZQs and BZBs sources, while the histogram in the background represents the normalized density of the distribution of the whole WFB sample along the  $PC_1$  axis. The horizontal green line shows the threshold used to determine the boundaries of the mixed region.

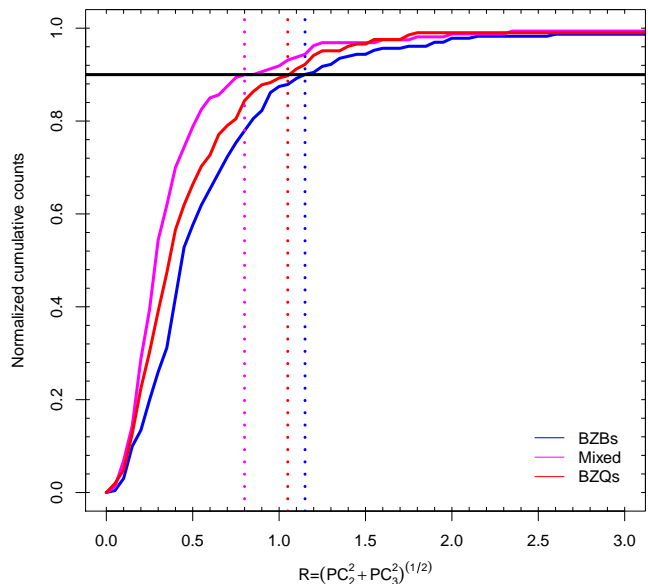


**Figure 4.** Cumulative radial profiles of the WFB sources for the three different sections of the model of the WFB *locus* in the PCs space. The red, magenta and blue solid lines represent the cumulative profiles of the WFB sources belonging to the BZQs, mixed and BZBs sections of the model, respectively. The horizontal black line shows the 90% threshold used to determine the radii of the three cylinders (dotted vertical lines).

**Table 2**

Parameters of the three cylinders representing the model of the WFB *locus* in the PCs space.

	BZB	Mixed	BZQ
PC <sub>1</sub> low.	-3.79	-0.24	0.92
PC <sub>1</sub> up.	-0.24	0.92	2.55
radius	1.15	0.8	1.05

The distance of a generic *WISE* source to the model of the WFB *locus* in the PCs space can be evaluated quantitatively using a numeric quantity that we call the score. The generic *WISE* source with colors  $(\tilde{c}_1, \tilde{c}_2, \tilde{c}_3)$  can be projected onto the PCs space by applying the orthogonal transformation determined by the PCA performed on the WFB sample for the modelization of the WFB *locus* in the PCs space (Section 3.1). Thus, the position of the generic *WISE* source in the PCs space is determined by the PCs values  $(PC_1, PC_2, PC_3) = T(\tilde{c}_1, \tilde{c}_2, \tilde{c}_3)$ . To take into account the uncertainties on the values of the *WISE* colors, the standard deviations on each color are also projected onto the PCs space and are used to define the error bars on the position of the source in the PCs space:  $(\pm\sigma_{PC_1}, \pm\sigma_{PC_2}, \pm\sigma_{PC_3}) = T(\pm\sigma_{\tilde{c}_1}, \pm\sigma_{\tilde{c}_2}, \pm\sigma_{\tilde{c}_3})$ . We simply assume that the generic *WISE* source is represented in the PCs space by the ellipsoid generated by the segments with extremes  $PC_i \pm \sigma_{PC_i}$ , hereinafter the uncertainty ellipsoid. Each of the six points at the extremes of the axes of the uncertainty ellipsoid in the PCs space will be generically called extremal point. The possible positions of the uncertainty ellipsoid associated with a generic *WISE* source relative to each of the three cylinders of the *locus* model (schematically shown in Figure 5 for one two-dimensional section of the PCs space) fall in one of the following cases:

- Six extremal points within a cylinder (point A in Figure 5);
- Five extremal points within a cylinder (point B in Figure 5);
- Three extremal points within a cylinder (point C in Figure 5);
- One extremal point within a cylinder (points D in Figure 5);
- No extremal points within any cylinder (points F in Figure 5);

Other combinations are not possible because the axes of the uncertainty ellipsoids are either parallel or orthogonal to the PC<sub>1</sub> axis of the PCs space. Points with any number of extremal points within two cylinders (like point E in Figure 5) are assigned a distinct score value for either cylinder according to the number of extremal points contained in each one.

The score  $s$  for a generic *WISE* source with  $n$  extremal points contained in one of the three sections of the WFB *locus* model is then defined as:

$$s = \frac{1}{6^\phi} \cdot n^\phi \quad (3)$$

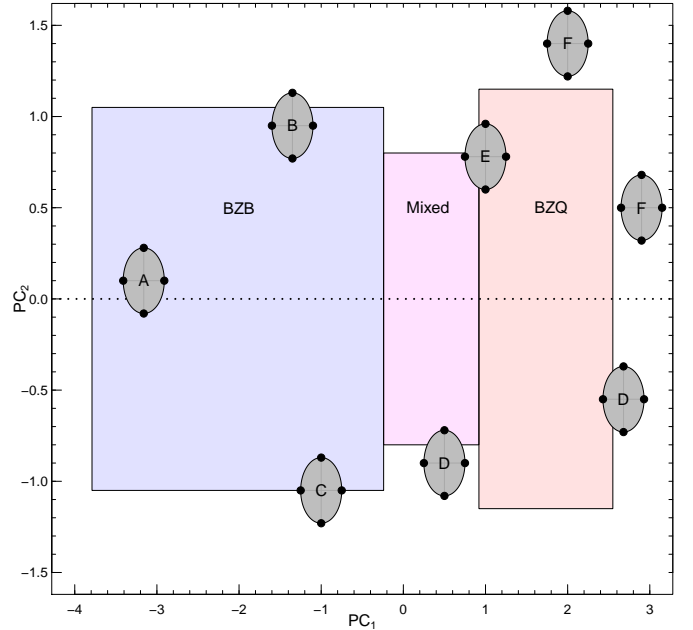


**Figure 5.** Schematic representation of the possible positions of the uncertainty ellipsoid of a generic *WISE* source in the PCs space relative to the cylindrical models of the WFB *locus*. In this plot the projection of the three-dimensional model and the uncertainty ellipsoids on a plane containing the axis of the cylinders are shown. The letters are references to the description of the different cases in Sec. 3.2.

where  $\phi$  is the *index* of the score assignment law. This is a simple generalization of the most natural choice that would assign to each extremal point within the *locus* model 1/6, defining the total score of a source as linearly proportional to the number of extremal points within the model cylinders. This behavior is obtained in the general equation when  $\phi=1$ . Changing the value of  $\phi$  is useful to tweak the performances of the association procedure in terms of the purity and completeness of the final sample of candidate blazars. While in this paper  $\phi=1$  will be used for all experiments, the discussion of the influence of the value of the parameter  $\phi$  on the results of the application of the association procedure and the justification of the choice of the value of  $\phi$  used in the experiments in this paper can be found in Appendix A.

So far, the score assigned to a generic *WISE* source can take one of six different values determined by the score assignment law in Equation 3. To penalize the *WISE* sources with large uncertainties on the observed colors (and, in turn, large volume of the uncertainty ellipsoid in the PCs space) relatively to other *WISE* sources with the same number of extremal points contained in the *locus* model but smaller errors, we multiply the score obtained using Equation 3 by the ratio of the absolute values of the logarithms of the volume of the uncertainty ellipsoid of the source considered and of the volume of the largest uncertainty ellipsoid for WFB sources. Thus, for each of the three regions of the *locus* model, the weighted score is defined as:

$$s_w = s \cdot \frac{\|\log V\|}{\|\log(\max(V_{\text{WFB}}))\|} \quad (4)$$

where  $V_{\text{WFB}}$  are the volumes of the uncertainty ellipsoids of the WFB sources in the PCs space calculated as  $V_{\text{WFB}} = \frac{4}{3}\pi\sigma_{\text{PC}_1}\sigma_{\text{PC}_2}\sigma_{\text{PC}_3}$ , and  $V$  is the volume of the uncertainty ellipsoid in the PCs space of the generic *WISE* source considered. The logarithms of the volumes of the uncertainty ellipsoids are used to take into account the large number of order of magnitude potentially spanned by the differences between the volumes (always smaller than one in the PCs space though). The above definition of the weighted score also has the effect of mapping the discrete distribution of scores calculated according to assignment law Equation 3 into a continuous distribution that allows a finer classification of the candidate blazars (as described in Section 4.1). In the remainder of the paper the term score will always be used to indicate the weighted score definition given in Equation 4.

#### 4. THE ASSOCIATION PROCEDURE

##### 4.1. Selection of the candidate blazars

The procedure for the evaluation of the scores based on the new parametrization of the WFB *locus* discussed in the previous section is used to associate high-energy sources to *WISE* candidate blazars. The *WISE* colors and their uncertainties for all the sources found in the *WISE* All-Sky photometry catalog within the region of positional uncertainty (hereinafter the Search Region - SR) of a given high-energy source and detected in all four *WISE* filters are retrieved, and the scores of these *WISE* sources are calculated as described in Section 3.2. Then, these sources are split among different classes according to the values of their scores  $s_b$ ,  $s_m$  and  $s_q$  for the BZB, Mixed and BZQ regions of the WFB *locus* model in the PCs space respectively. For each *locus* region, every source is assigned to class A, class B, class C or is marked as an outlier based on its score values and relative to the threshold scores values defined as the 30%, 60% and 90% percentiles of the distributions of scores in the three regions of the *locus* for the WFB sources (see Figure 6). The classes are sorted according to decreasing probability of the *WISE* source to be compatible with the model of the WFB *locus*: class A sources are considered the most probable candidate blazars for the high-energy source in the SR, while class B and class C sources are less compatible with the WFB *locus* but are still deemed as candidate blazars. In more details, class A candidate blazars have score  $s \leq s_{90\%}$ , class B candidate blazars have score  $s_{60\%} \leq s \leq s_{90\%}$  and class C candidate blazars have score  $s_{30\%} \leq s \leq s_{60\%}$  for each region. The other sources considered outliers are discarded. The values of the score thresholds derived from the score distributions of WFB sources for the three regions of the *locus* model are reported in Table 3 and shown in Figure 6 overplotted to the histograms of the score distributions of the WFB sources assigned to each of the three *locus* regions. The choice of the percentiles used to define the classes of candidate blazars is arbitrary and can be changed to allow for more conservative (higher purity of the sample of candidates) or more complete (lower purity of the sample of candidates) selections of candidate blazars in the SRs associated with unidentified high-energy sources.

##### 4.2. Background and spurious associations

In our association procedure, the presence of *WISE* background sources with score values that would qual-

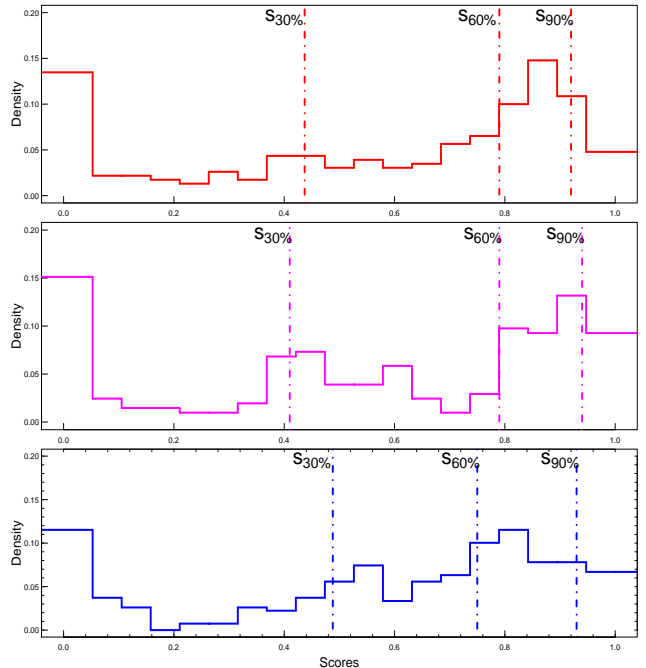


**Figure 6.** Histograms of distributions of score values calculated for the sources in the WFB sample for the three regions of the *locus* dominated respectively by the BZQs, the BZBs and in the mixed region (upper, mid and lower panels respectively). The three vertical lines in each panel represent  $s_{30\%}$ ,  $s_{60\%}$  and  $s_{90\%}$ , i.e. the values of the score associated with the 30%-th, 60%-th and 90%-th percentiles for BZBs, BZQs and mixed sources respectively. These score thresholds have been used to define the classes of candidate blazars (see Section 4 for details).

**Table 3**

Values of the score thresholds  $s_{30\%}$ ,  $s_{60\%}$  and  $s_{90\%}$ , used for the association experiments described in this paper. These values are determined as the 30%-th, 60%-th and 90%-th percentiles of the scores of the WFB sample divided by BZB, Mixed and BZQ mixed regions.

	BZB	Mixed	BZQ
$s_{30\%}$	0.48	0.44	0.41
$s_{60\%}$	0.75	0.79	0.79
$s_{90\%}$	0.93	0.92	0.94

ify them as candidate blazars but that are not located within the SR of the unidentified high-energy source is taken into account by assessing the number and type of spurious associations from sources within a local background region for each unassociated source. For a generic SR of radius  $r_{\text{SR}}$ , we define the background region (BR) as an annulus of outer radius  $r_{\text{BR}} = \sqrt{2} \cdot r_{\text{SR}}$  and inner radius equal to the SR radius and centered on the center of the SR. The SR and BR have same area by definition. Within a given SR, all *WISE* sources detected in all four *WISE* filters are assigned a score value for each region of the *locus* model, and successively ranked in classes using the same thresholds used to classify the sources within the SR. An example of a generic SR and associated background region is shown in Figure 7, where the candidate blazar and the spurious BR candidate blazar are colored according to their class membership as defined in Section 4.

For every unassociated high-energy source, our method

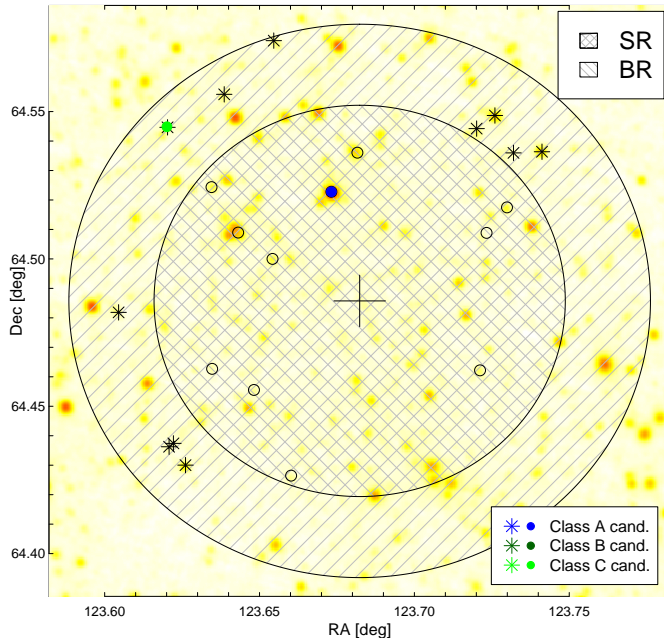


**Figure 7.** Results of the association procedure for a generic unassociated high-energy source superimposed on the image of the *WISE* sky around the position of the unassociated  $\gamma$ -ray source as seen in the  $[3.4]\mu\text{m}$  band. The inner circle represents the Search Region (SR) of the high-energy source while the outer circle delimits the annulus used as Background Region (BR). The open circles in the SR represent the sources of the *WISE* All-Sky catalog detected in all four *WISE* filters for which the scores have been evaluated (the sources not marked by symbols in the image are not detected in at least one of the four *WISE* filters and have not been considered for the score evaluation). The solid circle represents the candidate blazar found within the SR and its color indicates that it is class A candidate blazar. The gray stars in the background region are the *WISE* sources used to assess the possibility of spurious associations. Only one source in the BR has been classified as class C candidate blazar in this example.

produces all candidate blazars (sources classified as class A, class B or class C candidate) in the SR. All candidate blazars located in the BR of the high-energy sources are also provided and can be used to evaluate the chance of spurious associations as a function of the class of the candidate blazars (see, for example, Section 5 and Section 7 for WFB and 2FB association respectively, and the last columns of Table 5 and Table 7).

#### 5. RE-ASSOCIATION OF THE *WISE* GAMMA-RAY EMITTING BLAZARS

The association procedure based on the new model of the *locus* of the WFB in the 3-dimensional *WISE* color space (described in Sec. 3.1) has been applied to the  $\gamma$ -ray sources of the WFB sample. The candidate blazars have been classified according to the score thresholds described in Sec. 4 and shown in Table 3. The SR associated with each  $\gamma$ -ray source has been defined as a circular region of radius  $\theta_{95}$  corresponding to the semi-major axis of the uncertainty positional region at 95% level of confidence (see Nolan et al. 2012, for additional details). The method finds 542 candidate blazars for 486 out of 610 WFB  $\gamma$ -ray sources, corresponding to  $\sim 80\%$  of the WFB sample. The 542 candidate blazars are divided into 186 BZB candidate blazars, 165 candidate blazars compatible with the Mixed region and the remaining 191 BZQ candi-

**Table 4**

Composition of the samples of candidate blazars selected by applying our association method to the  $\gamma$ -ray sources in the WFB and 2FB samples in terms of candidate types and class. See Section 5 and Section 7 for more details on the re-association of the WFB sample and the association of the 2FB sample respectively.

	WFB		
	Class A	Class B	Class C
BZB	28	81	77
Mixed	23	59	83
BZQ	24	71	96
	2FB		
	Class A	Class B	Class C
BZB	0	13	5
Mixed	4	13	9
BZQ	4	8	20

date blazars. The 542 candidate blazars are distributed in 75 class A candidates, 211 class B candidates and 256 class C candidate blazars. The average number of candidate blazars for each associated WFB  $\gamma$ -ray source is  $\sim 1.1$ , with 197 WFB sources associated with only one *WISE* candidate. Out of the total of 486  $\gamma$ -ray sources in the WFB that have been associated with at least one *WISE* candidate blazar, 468 sources have been associated (among other possible candidate blazars selected) to the same *WISE* source which has been selected as the counterpart of the  $\gamma$ -ray source according to the analysis discussed in Section 2.3, corresponding to  $\sim 77\%$  of the WFB sample. More details on this topic are given in Section 6 where the evaluation of the efficiency and completeness of the association procedure is discussed. A summary of the composition of the sample of candidate blazars selected by the new association method applied to the WFB sample can be found in Table 4.

Table 5 shows the basic information for the first ten candidate blazars of the WFB sample that have been re-associated with the same *WISE* counterparts used in the WFB catalog itself. The complete list of candidate blazars associated with the WFB sources can be found in the Table 8 in Appendix B.

Table 6 shows some basic information for the first ten candidate blazars associated with the WFB sample but representing alternative associations of the  $\gamma$ -ray sources in the WFB sample (i.e., different *WISE* sources from the counterparts identified for the WFB sample with the positional method described in Section 2.2). For each of these candidate blazars, an extensive archival research has been performed in order to gather all critical information useful to characterize the nature of the source. This information is reported in the tenth column of Table 6, summarizing the available classifications and detections in different observations for each alternative association. The last column of this Table also reports the total number of BR candidate blazars, determined as described in Section 4.2, with class higher than or equal to the class of the candidate blazars associated with the  $\gamma$ -ray source and located within its SR. No class A candidate blazars have been found within the BRs of the 75 WFB sources associated to at least one class A candidate blazar (0%), while 32 out of the 201 WFB sources associated to a class B candidate have at least one class B or better candidate blazar in the BR ( $\sim 16\%$ ). Finally, 167 out of the remain-

**Table 5**

First ten *WISE* candidate blazars associated to WFB sources and corresponding to the association in the 2FGL catalog (the complete list of WFB associations can be found in Table 8 in Appendix B).

2FGL <sup>a</sup> name	<i>WISE</i> <sup>b</sup> name	ROMA-BZCAT <sup>c</sup> name	[3.4]-[4.6] <sup>d</sup> mag	[4.6]-[12] <sup>e</sup> mag	[12]-[22] <sup>f</sup> mag	z <sup>g</sup>	type <sup>h</sup>	class <sup>i</sup>
2FGLJ0000.9-0748	J000118.01-074626.7	BZBJ0001-0746	0.93(0.03)	2.53(0.04)	2.12(0.1)	?	BZB	B
2FGLJ0004.7-4736	J000435.64-473619.5	BZQJ0004-4736	1.09(0.03)	2.92(0.03)	2.3 (0.06)	0.88	UND	C
2FGLJ0006.1+3821	J000557.17+382015.2	BZQJ0005+3820	1.1 (0.03)	3.11(0.03)	2.69(0.03)	0.229	BZQ	A
2FGLJ0007.8+4713	J000759.97+471207.7	BZBJ0007+4712	0.92(0.04)	2.28(0.06)	2.13(0.18)	0.28	BZB	C
2FGLJ0012.9-3954	J001259.88-395425.8	BZBJ0012-3954	1.01(0.04)	2.84(0.04)	2.28(0.11)	?	UND	C
2FGLJ0013.8+1907	J001356.36+191042.0	BZBJ0013+1910	0.97(0.04)	2.58(0.06)	2.09(0.22)	?	BZB	C
2FGLJ0017.6-0510	J001735.81-051241.6	BZQJ0017-0512	1.06(0.03)	2.73(0.04)	2.45(0.08)	0.227	UND	B
2FGLJ0021.6-2551	J002132.54-255049.2	BZBJ0021-2550	0.85(0.04)	2.3 (0.06)	2.23(0.1)	?	BZB	C
2FGLJ0022.5+0607	J002232.44+060804.4	BZBJ0022+0608	1.04(0.03)	2.8 (0.04)	2.28(0.09)	?	UND	B
2FGLJ0023.2+4454	J002335.44+445635.8	BZQJ0023+4456	1.22(0.04)	2.92(0.06)	2.41(0.14)	1.062	BZQ	C

Notes:

<sup>a</sup> 2FLG name of the  $\gamma$ -ray source associated

<sup>b</sup> *WISE* name of the candidate blazars

<sup>c</sup> ROMA-BZCAT name of the source

<sup>d</sup>  $c_1$  *WISE* color of the candidate

<sup>e</sup>  $c_2$  *WISE* color of the candidate

<sup>f</sup>  $c_3$  *WISE* color of the candidate

<sup>g</sup> redshift of the ROMA-BZCAT source

<sup>h</sup> classification of the candidate blazar according to our method

<sup>i</sup> class of the candidate blazar according to our method

ing 192 WFB sources associated to a class C candidate blazar have at least one candidate blazar of equal or better class in their BRs ( $\sim 87\%$ ), confirming that class C candidate blazars are the most sensitive to possible contamination from background *WISE* sources compatible with the *locus* model. The complete list of alternative associations of the WFB sources can be found in Table 8 in Appendix B.

## 6. EFFICIENCY AND COMPLETENESS

The new parametrization of the *locus*, coupled with the revisited association procedure described in Section 4, can be treated as a *classifier* whose parameters are optimized through a supervised learning procedure. The training sample of this classifier is the WFB sample that has been used to define the *locus* model in the PCs space generated by the WFB distribution in the *WISE* color space, because the association procedure is based on the geometry of the *locus*. More specifically, the training of the classifier consists in the characterization of the *locus* model that is used to calculate the scores and to select the candidate blazars. In general, after a classifier has been trained its performances can be evaluated by applying the trained classifier on a different sample of sources, the testset, representative of the same underlying population from where the training set has been extracted. The performance of a classification method can be expressed by two quantities, the efficiency and the completeness of the classification. The efficiency is the ratio between the number of sources correctly classified by the classifier in the test-set and the total number of sources classified, and the completeness is the fraction of sources that the method correctly classifies relative to the total number of sources in the test-set that would have been correctly classified by an ideal perfect classifier.

The classification performed by the association procedure on one  $\gamma$ -ray source of the WFB sample is considered correct if one of the *WISE* sources associated with the WFB  $\gamma$ -ray source is the *WISE* source identified as counterpart of the WFB source by the method described

in Section 2)<sup>10</sup>. The efficiency  $e$  and completeness  $c$  are thus defined as:

$$e = \frac{n(\text{Correctly associated } \gamma\text{-ray sources})}{n(\text{Associated } \gamma\text{-ray sources})}$$

$$c = \frac{n(\text{Correctly associated } \gamma\text{-ray sources})}{n(\gamma\text{-ray sources to be associated})}$$

When the size of the parent population of the sample of sources used to train and test the classifier is large enough, training set and testset can be obtained by splitting the parent population in two subsets of different sizes. The minimum size of the sample that would permit to apply this strategy depends on the specific problem, on the features of the classifier used and the sample itself. Common choices of the training set to testset size proportions are 60%-40% or 70%-30%. Using this approach to assess the performances of our classifier, we verified that the values of the efficiency and completeness of the association strongly depended on the composition of both samples, revealing a suboptimal training of the classifier that led to “over-fitting”. Two likely causes of this behavior are, respectively, that our classifier is too complex to be trained on 60% or 70% fraction of the WFB sample, and that the parameters of the *locus* model are very sensitive to the particular subset of sources contained in the training test. To avoid this issue, we have used all WFB sources to determine the *locus* modelization, as described in Section 3, and estimated the efficiency  $e$  and completeness  $c$  of the association procedure using a different strategy, the  $K$ -fold cross-validation Hastie et al. (2009), that employs the same sample used as train-

<sup>10</sup> The candidate blazars that do not correspond to the *WISE* counterparts of the blazars in the WFB sample do not necessarily are incorrect from the physical point of view, as they can possibly represent more physically meaningful associations of the high-energy source worth further investigation. We label them as “incorrect” only to simplify the description of the evaluation of the efficiency and completeness of the association procedure.



Table 6

First ten candidate blazars associated to WFB sources that do not correspond to the *WISE* counterparts of the associations in the 2FLG catalog (the complete list of WFB associations can be found in Table 8 in Appendix B).

2FGL <sup>a</sup> name	<i>WISE</i> <sup>b</sup> name	other <sup>c</sup> name	[3.4]-[4.6] <sup>d</sup> mag	[4.6]-[12] <sup>e</sup> mag	[12]-[22] <sup>f</sup> mag	type <sup>g</sup>	class <sup>h</sup>	notes <sup>i</sup>	$z^l$	$N_{BR}^m$
2FGLJ0000.9-0748	J000115.93-074233.1	APMUKS(BJ) B235842.09-075916.3	1.03(0.05)	3.21(0.08)	2.45(0.20)	BZQ	C	-	-	1
2FGLJ0007.8+4713	J000745.11+471130.7	NVSSJ000745+471131	1.15(0.06)	2.92(0.12)	2.68(0.27)	BZQ	C	N,X	-	0
2FGLJ0102.3+4216	J010142.98+421828.3	GALEXJ010142.98+421828.4	1.00(0.05)	2.76(0.09)	2.40(0.28)	UND	C	-	-	1
2FGLJ0116.0-1134	J011559.75-113012.3	GALEX2673671438794228469	1.13(0.03)	2.46(0.03)	2.36(0.05)	UND	C	M	-	1
2FGLJ0158.3-3931	J015752.11-392906.2		1.17(0.04)	3.19(0.05)	2.58(0.11)	BZQ	C	M	-	1
2FGLJ0205.4+3211	J020537.46+321812.7		0.96(0.04)	2.58(0.06)	2.38(0.16)	UND	C	M	-	1
2FGLJ0217.5-0813	J021649.93-080551.8	SDSSJ021649.94-080551.8	1.11(0.04)	3.23(0.05)	2.45(0.12)	BZQ	C	s	-	3
2FGLJ0217.5-0813	J021716.20-082816.2	SDSSJ021716.21-082816.3	1.19(0.03)	2.68(0.03)	2.35(0.04)	UND	C	M	0.497	3
2FGLJ0219.1-1725	J021906.91-173135.3		1.20(0.05)	2.98(0.09)	2.37(0.25)	BZQ	C	-	-	2
2FGLJ0222.0-1615	J022222.65-162309.6		1.11(0.06)	3.04(0.10)	2.68(0.24)	BZQ	C	-	-	0

Notes:

<sup>a</sup> 2FGL name of the  $\gamma$ -ray source associated

<sup>b</sup> *WISE* name of the candidate blazars

<sup>c</sup> alternative name (if available) of the source in the literature

<sup>d</sup>  $c_1$  *WISE* color of the candidate

<sup>e</sup>  $c_2$  *WISE* color of the candidate

<sup>f</sup>  $c_3$  *WISE* color of the candidate

<sup>g</sup> classification of the candidate blazar according to our method

<sup>h</sup> class of the candidate blazar according to our method

<sup>i</sup> note about the available multi-wavelength information of the *WISE* source, if already observed and/or classified (surveys: N=NVSS, F=FIRST, S=SUMSS, M=2MASS, s=SDSS DR8, 6=6dFG, x=XMM or *Chandra*, X=ROSAT; classification: QSO=quasar, Sy=Seyfert, LNR=LINER; variability: v=variable in *WISE* (var\_flag > 5 in at least one *WISE* filter))

<sup>l</sup> redshift of the sources

<sup>m</sup> number of *WISE* sources in the background region (BR) of the  $\gamma$ -ray source selected as candidate blazars with class equal or higher than the class of the best candidate blazar selected in the SR of the high-energy source.

ing set. With the  $K$ -fold cross-validation approach, the WFB sample is randomly partitioned into  $K$  equal sized subsamples. Of the  $K$  subsamples, only one subsample is retained as the testset data to evaluate the performances of the association procedure, while the remaining  $K - 1$  subsamples are used as training data of the *locus* model. Thus the efficiency and completeness are evaluated on the  $K$ -th subset not used for training. The same steps are then repeated  $K$  times, with each of the  $K$  subsets of the WFB sample used exactly once as testset. The efficiency and completeness values determined for each of the  $K$  cross-validations can be combined to produce single robust estimates.

The parameters of the  $K$  different models of the *locus* estimated with the cross-validation on the sum of the  $K-1$  subsets not used for validation are compatible with the values obtained with the procedure described in Section 3.1 for  $K = \{20, 30, 50, 100\}$ . The total efficiency and completeness for the re-association of the WFB sources performed with the new association procedure are  $e_{\text{tot}} \simeq 97\%$  and  $c_{\text{tot}} \simeq 81\%$  respectively. Both  $e$  and  $c$  have been also estimated as functions of the *WISE* colors and the galactic coordinates of the *WISE* sources (Figure 8 for the efficiency maps and Figure 9 for the completeness maps). The maps of  $e$  and  $c$  in the color-color planes and galactic coordinates have been created by estimating the two quantities in bins of the three independent *WISE* color-color projections and galactic coordinates respectively. For example, the efficiency  $e_{ij}^{(c_1 c_2)}$  and completeness  $c_{ij}^{(c_1 c_2)}$  evaluated in the  $ij$ -th bin of the first *WISE* color-color plane are defined as:

$$e_{ij}^{(c_1 c_2)} = e(c_1(i) \leq c_1 < c_1(i+1), c_2(i) \leq c_2 < c_2(i+1))$$

$$c_{ij}^{(c_1 c_2)} = c(c_1(i) \leq c_1 < c_1(i+1), c_2(i) \leq c_2 < c_2(i+1))$$

Similarly, we evaluate  $e$  and  $c$  in the  $ij$ -th bin of the galactic coordinates distribution of the WFB *WISE* counterparts as follows:

$$e_{ij}^{(lb)} = e(l_1(i) \leq l < l(i+1), b(i) \leq b < b(i+1))$$

$$c_{ij}^{(lb)} = c(l_1(i) \leq l < l(i+1), b(i) \leq b < b(i+1))$$

The plots in Figure 8 and Figure 9 show the values of the normalized efficiency and completeness expressed as the color of the symbols, while the size of the symbols are proportional to the total number of  $\gamma$ -ray candidate blazars falling in each bin of the maps. The right lower plots in both figures show the values of  $e$  and  $c$  as functions of the galactic coordinates in Aitoff projection. One comment that can be made by observing the efficiency map in galactic coordinates in the lower-right plot in Figure 8 is that the contribution of galactic sources to the contamination of the association procedure is not dominant as there is no clear indication of a positive gradient of the efficiency as a function of the galactic latitude (namely, going from the galactic disk to the galactic north and south poles).

## 7. ASSOCIATION OF THE FERMI GAMMA-RAY BLAZARS

The sample of  $\gamma$ -ray blazars associated by the 2FGL contains 752  $\gamma$ -ray sources, excluding all sources with any analysis flag. We excluded from this list the 610 blazars already contained in WFB sample, for a final number of 142 2FGL sources. These  $\gamma$ -ray sources constitute the 2FGL *Fermi* blazar sample (hereinafter 2FB). The 2FB sample has been investigated with our association procedure similarly at what done for the WFB sample. The *locus* model and the parameters of the association procedure applied to the 2FB are the same used for the re-association of the WFB sample. The first ten associations of the 2FB sources are shown in Table 7, while the summary of the composition of the sample of candidate blazars associated with the 2FB sources can be found in Table 4. We summarize in the following the number and type of spurious candidate blazars found in the BRs of the 2FB sources. No class A spurious candidate blazars have been found within the BRs of the 8 2FB sources associated to at least one class A candidate blazar (0%),

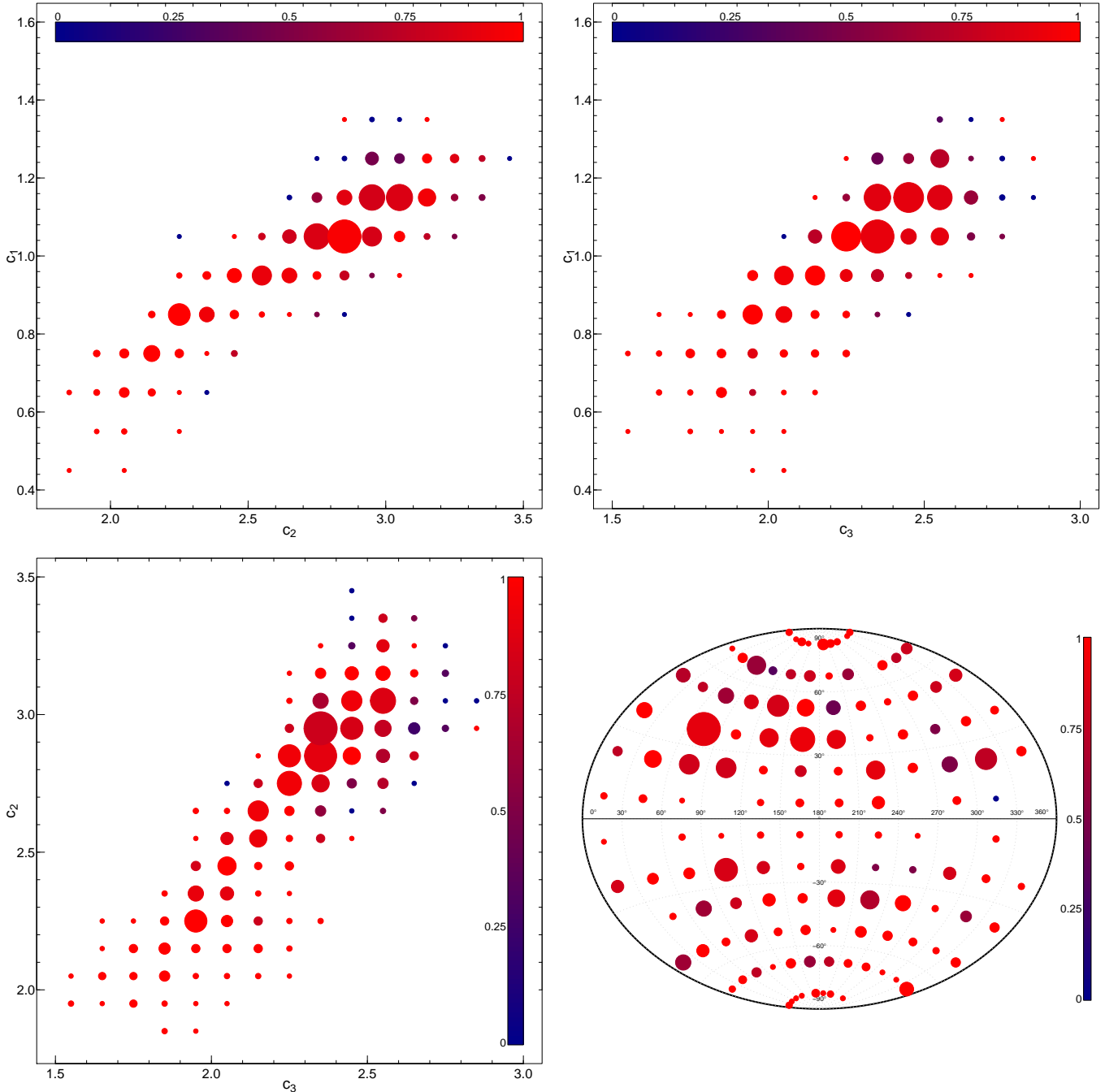


**Figure 8.** Maps of the efficiency  $e$  of the association procedure based on the new model of the WFB *locus* in the *WISE* color space obtained with the 100-fold cross-validation as described in Sec. 6. The upper-left plot shows  $e$  in the  $[3.4] - [4.6]$  vs  $[4.6] - [12]$  color-color plane, the upper-right plot shows  $e$  in the  $[4.6] - [12]$  vs  $[12] - [22]$  color-color plane and the lower-right plot shows  $e$  in the  $[3.4] - [4.6]$  vs  $[12] - [22]$  color-color plane. The lower-right plot shows the efficiency as a function of the galactic coordinates of the  $\gamma$ -ray sources in the WFB sample. In all plots, the size of the symbols is proportional to the number of WFB sources in the each bin and the local value of the efficiency normalized to unity is color-coded.

only 1 out of the 34 2FB sources associated to a class B or better candidate has one class B candidate blazar in the BR ( $\sim 3\%$ ). The number of 2FB sources associated to class C candidate blazars with at least one candidate blazars of same or better class is 31 out of the remaining 34 sources, corresponding to the  $\sim 91\%$  of this sample. Also in this case, an extensive archival research has been performed for all candidate blazars associated by our method. This research has led to gather the essen-

tial information about the candidate blazars contained in the tenth column of Table 7.

## 8. SUMMARY AND CONCLUSIONS

Using the preliminary data release of the Wide-field Infrared Survey Explorer (*WISE*), we discovered that  $\gamma$ -ray emitting blazars have infrared colors that distinguish them from other galactic and extragalactic sources in the 3-dimensional IR color space (Papers I and II). Then, we used these results to develop an association method able

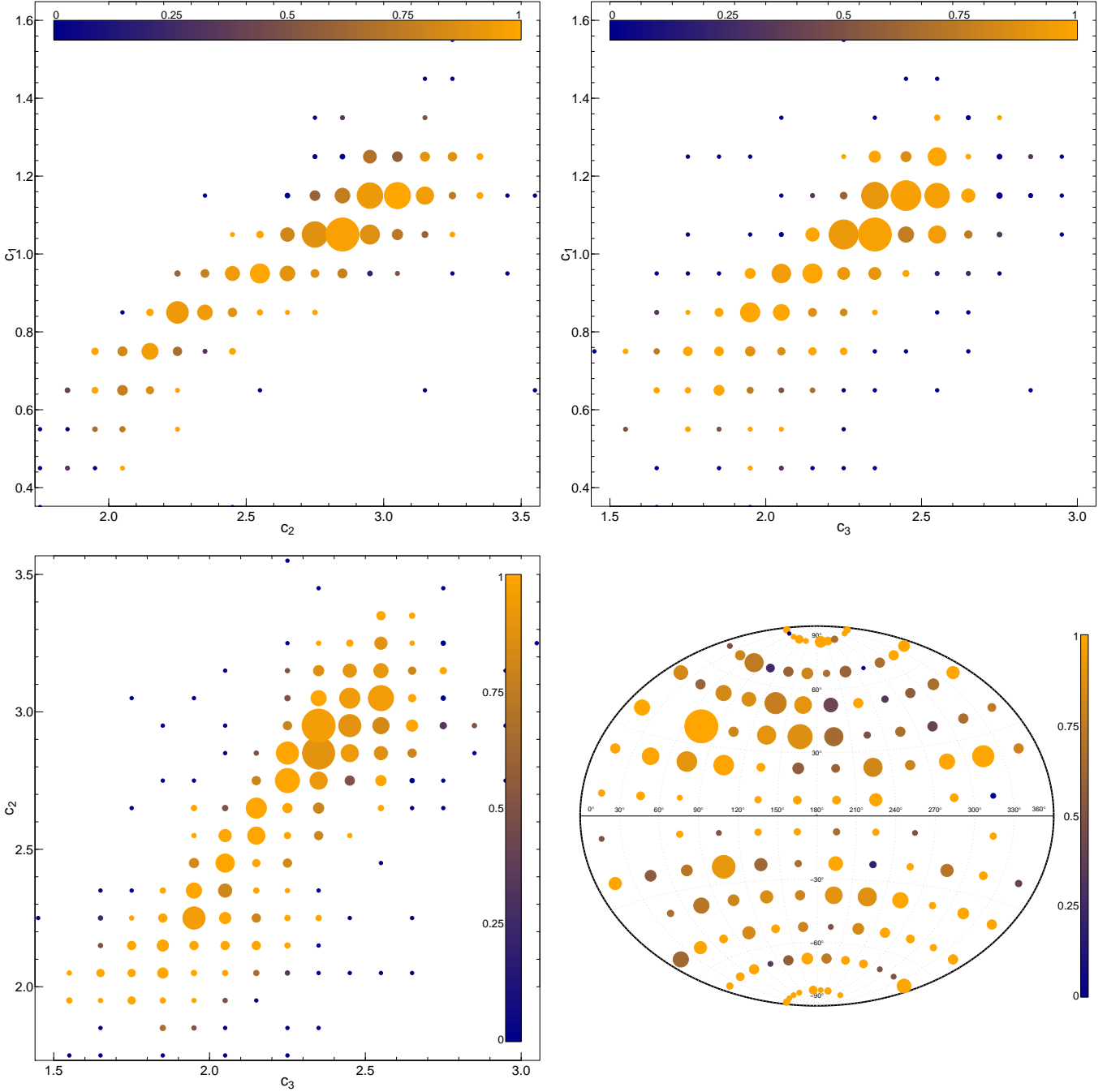


**Figure 9.** Maps of the completeness  $c$  of the association procedure based on the new model of the WFB *locus* in the *WISE* color space obtained with the 100-fold cross-validation as described in Sec. 6. The upper-left plot shows  $c$  in the  $[3.4] - [4.6]$  vs  $[4.6] - [12]$  color-color plane, the upper-right plot shows  $c$  in the  $[4.6] - [12]$  vs  $[12] - [22]$  color-color plane and the lower-right plot shows  $c$  in the  $[3.4] - [4.6]$  vs  $[12] - [22]$  color-color plane. The lower-left plot shows the completeness as a function of the galactic coordinates of the  $\gamma$ -ray sources in the WFB sample. In all plots, the size of the symbols is proportional to the number of WFB sources in the each bin and the local value of the efficiency normalized to unity is color-coded.

to associate IR selected blazar candidates as low-energy counterparts of a  $\gamma$ -ray source (Papers III and IV).

In this paper we have described an updated version of the WFB sample, gathered using the new *WISE* All-Sky release, the 2FGL catalog and the latest release of the ROMA-BZCAT list of blazars. Then, we have discussed a new association procedure for the unidentified high-energy sources based on a new model of the *locus* occupied by WFB sample in the three-dimensional PCs space

generated by the distribution of WFB *WISE* sources in the *WISE* color space. We defined a quantitative measure of the compatibility of a generic *WISE* source with the *locus* model and expounded the new association procedure. The new association procedure can select candidate blazars classified as BZB or BZQ candidates, and ranked according to the likelihood of each candidate of being an actual blazar. We also investigated the possibility of spurious associations by determining the number

Table 7

First ten candidate blazars associated to 2FB sources (the complete list of 2FB associations can be found in Table 9 in Appendix B).

2FGL <sup>a</sup> name	WISE <sup>b</sup> name	other <sup>c</sup> name	[3.4]-[4.6] <sup>d</sup> mag	[4.6]-[12] <sup>e</sup> mag	[12]-[22] <sup>f</sup> mag	type <sup>g</sup>	class <sup>h</sup>	notes <sup>i</sup>	z <sup>l</sup>	reassoc. <sup>m</sup> flag	N <sub>BR</sub> <sup>n</sup>
2FGLJ0035.8+5951	J003552.62+595004.3	BZBJ0035+5950	0.59(0.03)	2.03(0.03)	1.87(0.09)	BZB	B	M,v (0.08)6?	y	0	
2FGLJ0047.2+5657	J004700.43+565742.4	BZUJ0047+5657	1.03(0.04)	2.56(0.06)	2.4(0.13)	UND	C	v	0.747	y	1
2FGLJ0057.9+3311	J005832.05+331117.3	BZUJ0058+3311	1.13(0.05)	3.0(0.07)	2.45(0.19)	BZQ	C	-	1.369	y	4
2FGLJ0102.7+5827	J010245.75+582411.1	BZUJ0102+5824	1.06(0.03)	2.98(0.03)	2.45(0.05)	BZQ	C	v	0.644?	y	0
2FGLJ0105.3+3930	J010509.20+392815.2	BZUJ0105+3928	1.01(0.03)	2.5(0.03)	2.16(0.05)	UND	C	v (0.08)3?	y	1	
2FGLJ0105.3+3930	J010542.74+393024.2	-	1.17(0.06)	3.14(0.1)	2.55(0.26)	BZQ	C	-	?	n	-
2FGLJ0109.9+6132	J010946.32+613330.4	NVSSJ010946+613329	1.06(0.03)	2.71(0.03)	2.47(0.05)	UND	B	v	0.783	y	0
2FGLJ0113.2-3557	J011315.83-355148.2	BZQJ0113-3551	1.12(0.04)	2.9(0.05)	2.48(0.1)	BZQ	C	-	1.22	y	2
2FGLJ0114.7+1326	J011452.77+132537.6	BZBJ0114+1325	0.82(0.03)	2.3(0.04)	1.86(0.15)	BZB	B	M	?	y	0
2FGLJ0144.6+2704	J014433.54+270503.1	BZUJ0144+2705	1.07(0.03)	2.75(0.03)	2.22(0.04)	UND	B	M,v	?	y	0

Notes:

<sup>a</sup> 2FGL name of the  $\gamma$ -ray source associated<sup>b</sup> WISE name of the candidate blazars<sup>c</sup> alternative name (if available) of the source in the literature<sup>d</sup>  $c_1$  WISE color of the candidate<sup>e</sup>  $c_2$  WISE color of the candidate<sup>f</sup>  $c_3$  WISE color of the candidate<sup>g</sup> classification of the candidate blazar according to our method<sup>h</sup> class of the candidate blazar according to our method<sup>i</sup> note about the available multi-wavelength information of the WISE source, if already observed and/or classified (surveys: N=NVSS, F=FIRST, S=SUMSS, M=2MASS, s=SDSS DR8, 6=6dFG, x=XMM or *Chandra*, X=ROSAT; classification: QSO=quasar, Sy=Seyfert, LNR=LINER; variability: v=variable in WISE (var\_flag > 5 in at least one WISE filter))<sup>l</sup> redshift of the sources<sup>m</sup> flag indicating whether our association corresponds to the association provided in the 2FGL catalog (“y”), or otherwise (“n”)<sup>n</sup> number of WISE sources in the background region (BR) of the  $\gamma$ -ray source selected as candidate blazars with class equal or higher than the class of the best candidate blazar selected in the SR of the high-energy source.

and class of WISE sources compatible with the model of the WFB *locus* in background regions defined around the SR of each high-energy source. We have assessed the performances of the association procedure in terms of the efficiency and completeness by re-associating the  $\gamma$ -ray sources in the WFB sample, yielding a total efficiency  $e_{\text{tot}} \simeq 97\%$  and total completeness  $c_{\text{tot}} \simeq 81\%$  respectively. By using a  $K$ -fold cross-validation approach, we have also estimated the efficiency and completeness as functions of the WISE colors and galactic coordinates of the candidate blazars. The lack of a positive gradient in the efficiency of the association procedure as function of the galactic latitude suggests that galactic sources do not contribute significantly to the contamination of the *locus*. We will make the code for the association procedure available to the astronomical community on request.

In this paper, we have presented the catalog of candidate blazars associated by the new procedure to the 2FGL  $\gamma$ -ray sources included in the WFB sample, used to define the new model of the *locus*. We have investigated the archival information available for the WISE sources representing alternative associations of the *Fermi*  $\gamma$ -ray sources in the WFB. We also presented the catalog of candidate blazars obtained by applying the new association procedure to the 2FB sample, composed of all clean  $\gamma$ -ray sources associated with blazars in the 2FGL catalog but not contained in the WFB sample. In both catalogs, for every candidate blazar we provided the basic WISE data and information about the association; for the alternative associations (candidate blazars different from the WISE counterparts defined in the WFB and 2FB samples), we complemented the WISE data with some additional archival information (known name and classification), when available, that can hopefully help to physically characterize the nature of these sources. We will make both catalogs publicly available in electronic format.

Finally, we acknowledge that the effects of the distribution in redshift and the variability in WISE observations of the WFB sources on the definition of the model of the *locus* on which the association procedure is based

are still unknown. To address these open questions, we plan to carry out a detailed investigation of the WISE blazar variability and the statistical characterization of the SEDs of WFB blazars, that will be presented in future papers.

The work is supported by the NASA grants NNX10AD50G, NNH09ZDA001N and NNX10AD68G. R. D’Abrusco gratefully acknowledges the financial support of the US Virtual Astronomical Observatory, which is sponsored by the National Science Foundation and the National Aeronautics and Space Administration. F. Massaro is grateful to A. Cavaliere, S. Digel, D. Harris, D. Thompson, A. Wehrle for their helpful discussions. The work by G. Tosti is supported by the ASI/INAF contract I/005/12/0. H. A. Smith acknowledges partial support from NASA/JPL grant RSA 1369566. TOPCAT<sup>11</sup> (Taylor 2005) and SAOImage DS9 were used extensively in this work for the preparation and manipulation of the tabular data and the images. This research has made use of data obtained from the High Energy Astrophysics Science Archive Research Center (HEASARC) provided by NASA’s Goddard Space Flight Center; the SIMBAD database operated at CDS, Strasbourg, France; the NASA/IPAC Extragalactic Database (NED) operated by the Jet Propulsion Laboratory, California Institute of Technology, under contract with the National Aeronautics and Space Administration. Part of this work is based on archival data, software or on-line services provided by the ASI Science Data Center. This publication makes use of data products from the Wide-field Infrared Survey Explorer, which is a joint project of the University of California, Los Angeles, and the Jet Propulsion Laboratory/California Institute of Technology, funded by the National Aeronautics and Space Administration.

## REFERENCES

Abdo, A. A. et al. 2010a ApJS 188 405

<sup>11</sup> <http://www.star.bris.ac.uk/~mbt/topcat/>

- Ackermann, M. et al. 2011 ApJ, 743, 171  
Ackermann, M. et al. 2012 ApJ, 753, 83  
Condon, J. J., Cotton, W. D., Greisen, E. W., Yin, Q. F., Perley, R. A., Taylor, G. B., & Broderick, J. J. 1998, AJ, 115, 1693  
D’Abrusco, R., Massaro, F., Ajello, M., Grindlay, J. E., Smith, Howard A. & Tosti, G. 2012 ApJ, 748, 68 (Paper II)  
Draine, B. T. 2003, ARA&A, 41, 241  
Hartman, R.C. et al., 1999 ApJS 123  
Hassan, T., Mirabal, N., Contreras, J. L., & Oya, I. 2013, MNRAS, 428, 220  
Hastie, T., Tibshirani, R., & Friedman, J. 2009, *The Elements of statistical learning*, Springer.  
Kovalev, Y. Y., Aller, H. D., Aller, M. F., et al. 2009, ApJ, 696, L17  
Kovalev, Y. Y. 2009, ApJ, 707, L56  
Maselli, A., Massaro, E., Nesci, R., Sclavi, S., Rossi, C., Giommi, P. 2010 A&A, 512A, 74  
Maselli, A., Cusumano, G., Massaro, E., La Parola, V., Segreto, A., Sbarufatti, B. 2010 A&A, 520A, 47  
Massaro, E., Giommi, P., Leto, C., Marchegiani, P., Maselli, A., Perri, M., Piranomonte, S., Sclavi, S. 2009 A&A, 495, 691  
Massaro, E., Giommi, P., Leto, C., Marchegiani, P., Maselli, A., Perri, M., Piranomonte, S., Sclavi, S. 2010 <http://arxiv.org/abs/1006.0922>  
Massaro, E., Giommi, P., Leto, C., Marchegiani, P., Maselli, A., Perri, M., Piranomonte, S., 2011 “Multifrequency Catalogue of Blazars (3rd Edition)”, ARACNE Editrice, Rome, Italy  
Massaro, F., D’Abrusco, R., Ajello, M., Grindlay, J. E. & Smith, H. A. 2011 ApJ, 740L, 48 (Paper I)  
Massaro, F., D’Abrusco, R., Tosti, G., Ajello, M., Gasparrini, D., Grindlay, J. E. & Smith, Howard A. 2012b ApJ, 750, 138 (Paper III)  
Massaro, F., D’Abrusco, R., Tosti, G., Ajello, M., Paggi, A., Gasparrini, 2012c ApJ, 752, 61(Paper IV)  
Massaro, F., D’Abrusco, R., Paggi, A., Tosti, G., Gasparrini, D. 2012d ApJ, 750L, 35 (Paper V)  
Mirabal, N. 2009 [arxiv.org/abs/0908.1389v2]  
Mirabal, N., & Halpern, J. P. 2009, ApJ, 701, L129  
Mirabal, Nieto, D. & Pardo, S. 2010 A&A submitted, [arxiv.org/abs/1007.2644v2]  
Nolan et al. 2012 ApJS, 199, 31  
Ruan, J. J., Anderson, S. F., MacLeod, C. L., et al. 2012, ApJ, 760, 51  
Stephen, J. B., Bassani, L., Malizia, A., et al. 2006, A&A, 445, 869  
Stickel, M., Padovani, P., Urry, C. M., Fried, J. W., Kuehr, H. 1991 ApJ, 374, 431  
Stern, D., Assef, R. J., Benford, D. J., et al. 2012, ApJ, 753, 30  
Stoeckel et al. 1991, ApJS, 76, 813  
Taylor, M. B. 2005, ASP Conf. Ser., 347, 29  
Urry, C. M., & Padovani, P. 1995, PASP, 107, 803  
Wright, E. L., et al. 2010 AJ, 140, 1868  
Yan, L., Donoso, E., Tsai, C.-W., et al. 2013, AJ, 145, 55

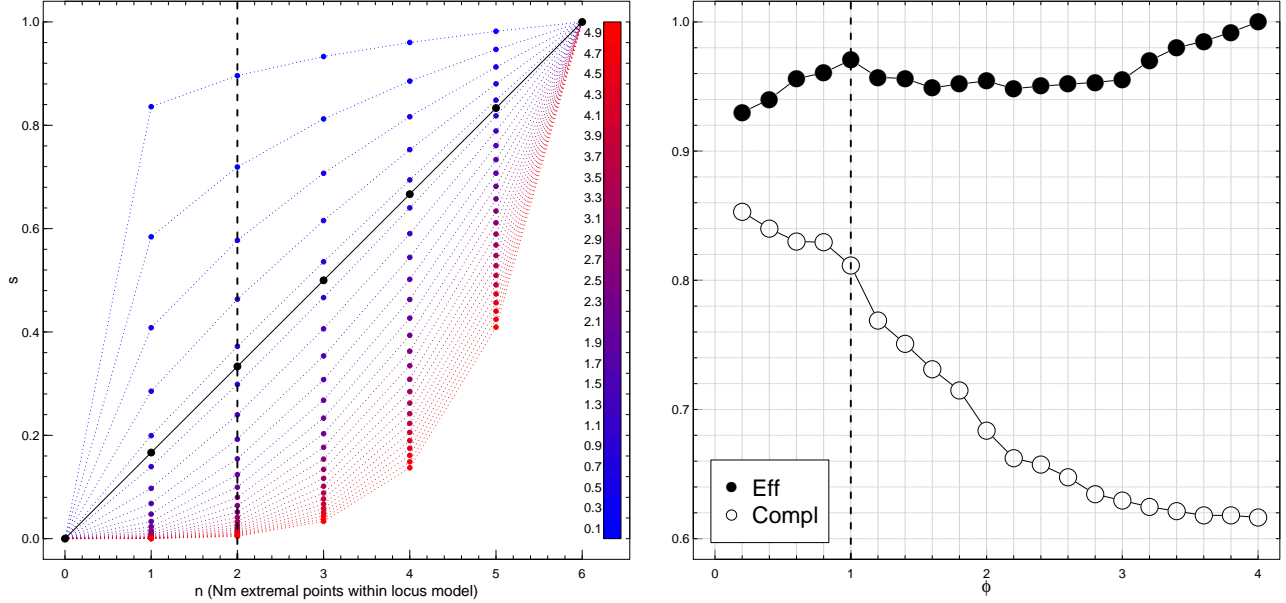


**Figure 10.** Left panel: score as function of the number of extremal points  $n$  contained in the *locus* model for different values of the parameter  $\phi$  of the score assignment law (Equation 3). For a fixed number of extremal points  $n$  within the model, the corresponding value of the score will be larger than  $n/6$  for  $\phi < 1$  and smaller than  $n/6$  for  $\phi > 1$  (the dashed vertical black line shows the score values for  $n = 2$  extremal points as an example). The linearly proportional assignment law for  $\phi = 1$  is represented by the curve with black solid circles. Right panel: Total efficiency  $e_{\text{tot}}$  (solid circles) and completeness  $c_{\text{tot}}$  (open circles) of the association procedure evaluated on the whole WFB sample as functions of the parameter  $\phi$  of the score assignment law (Equation 3 in Section 3.2). The values of  $e_{\text{tot}}$  and  $c_{\text{tot}}$  obtained with  $\phi = 1$ , used for the association of the WFB and 2FB samples in Section 5 and Section 7 respectively, are indicated by the vertical dashed line.

## 9. APPENDIX A: PERFORMANCES OF THE ASSOCIATION PROCEDURE AS FUNCTIONS OF INDEX OF THE SCORE ASSIGNMENT LAW

The score assignment law (Equation 3) has been introduced in Section 3.2 to provide a flexible way to assign the score values to the *WISE* sources as a function of the number of extremal points contained within the *locus* model. As shown in the left panel of Figure 10, the score of a source with  $n$  extremal points contained in one cylinder of the *locus* model for  $\phi > 1$  becomes smaller than the fractional value of  $1/n$ , while for  $\phi < 1$  the score becomes larger than the default value corresponding to the linear proportionality obtained with  $\phi = 1$ . The parameter  $\phi$  permits to control the behavior of the score assignment law and to tweak it for different scientific goals. For example, a more efficient (or pure) association can be obtained by assigning large score values only to the *WISE* sources with a large number of extremal points within the model; this can be accomplished by using a value of the index larger than unity. On the other hand, by assigning large scores to sources with few extremal points inside the model, the completeness of the selection can be enhanced at the cost of a lower efficiency. For this reason, the value of  $\phi$  has to be optimized for each distinct experiment. In the case of the experiments described in this paper, the choice of the value of the parameter  $\phi$  has been based on the characterization of the efficiency and completeness (defined in Section 6) of the association procedure as functions of  $\phi$ . We have run multiple association experiments on the WFB sample with fixed values of the parameters of the geometric model of the *locus* (see Table 2), but letting  $\phi$  vary in the  $(0.2, 4)$  range. Values of  $e_{\text{tot}}$  and  $c_{\text{tot}}$  have been evaluated for these experiments according to the definitions given in Section 6. The distributions of the  $e_{\text{tot}}$  and  $c_{\text{tot}}$  as functions of  $\phi$  are shown in the right panel in Figure 10.

The curve representing  $e_{\text{tot}}$  varies in the range  $(0.92, 1)$  but is not monotonically increasing with  $\phi$ . The total efficiency locally peaks at  $\sim 0.97$  for  $\phi = 1$  and then decreases to  $\sim 0.95$  for larger values of  $\phi$ . The plateau observed between  $\phi = 1.4$  and  $\phi = 1.3$  indicates that a large fraction of candidate blazars have a large number of extremal points within the cylindrical model of the *locus*, so that the slowly rising curve in the left panel in Figure 10 for small values of  $n$  and the steeper slope for  $n \geq 4$  do not affect the overall efficiency of the association. The efficiency becomes larger and then reaches 1 for  $\phi$  approaching 4. The total completeness  $c_{\text{tot}}$  is monotonically decreasing from small to large values of  $\phi$ , ranging from a maximum value  $\sim 0.85$  for  $\phi = 0.1$  to a minimum value of  $\sim 0.62$  for  $\phi = 4$ . In general, the value of  $\phi = 1$  used for the evaluation of the efficiency and completeness as functions of the color and galactic coordinates in Section 6 and the association of the WFB and 2FB samples has been chosen as a reasonable compromise between the largest achievable total efficiency and a large enough completeness for the association procedure applied on the WFB sample. Different experiments should be performed with values of the parameter  $\phi$  optimized for one aspect or the other of the association procedure.

APPENDIX B: COMPLETE LISTS OF *WISE* ASSOCIATIONS FOR WFB AND 2FB SAMPLES**Table 8** List of all candidate blazars associated to the WFB sources. The explanation of the content of the columns can be found in the notes of Table 5.

2FGL name	<i>WISE</i> name	ROMA-BZCAT name	[3.4]-[4.6] mag	[4.6]-[12] mag	[12]-[22] mag	z	type	class	$N_{BR}$
2FGLJ0000.9-0748	J000118.01-074626.7	BZBJ0001-0746	0.93(0.03)	2.53(0.04)	2.12(0.1)	?	BZB	B	0
2FGLJ0004.7-4736	J000435.64-473619.5	BZQJ0004-4736	1.09(0.03)	2.92(0.03)	2.3 (0.06)	0.88	UND	C	0
2FGLJ0006.1+3821	J000557.17+382015.2	BZQJ0005+3820	1.1 (0.03)	3.11(0.03)	2.69(0.03)	0.229	BZQ	A	0
2FGLJ0007.8+4713	J000759.97+471207.7	BZBJ0007+4712	0.92(0.04)	2.28(0.06)	2.13(0.18)	0.28	BZB	C	0
2FGLJ0012.9-3954	J001259.88-395425.8	BZBJ0012-3954	1.01(0.04)	2.84(0.04)	2.28(0.11)	?	UND	C	1
2FGLJ0013.8+1907	J001356.36+191042.0	BZBJ0013+1910	0.97(0.04)	2.58(0.06)	2.09(0.22)	?	BZB	C	1
2FGLJ0017.4-0018	J001611.08-001512.3	BZQJ0016-0015	1.29(0.11)	3.01(0.26)	3.65(0.33)	1.577	-	-	-
2FGLJ0017.6-0510	J001735.81-051241.6	BZQJ0017-0512	1.06(0.03)	2.73(0.04)	2.45(0.08)	0.227	UND	B	0
2FGLJ0021.6-2551	J002132.54-255049.2	BZBJ0021-2550	0.85(0.04)	2.3 (0.06)	2.23(0.1)	?	BZB	C	0
2FGLJ0022.5+0607	J002232.44+060804.4	BZBJ0022+0608	1.04(0.03)	2.8 (0.04)	2.28(0.09)	?	UND	B	0
2FGLJ0023.2+4454	J002335.44+445635.8	BZQJ0023+4456	1.22(0.04)	2.92(0.06)	2.41(0.14)	1.062	BZQ	C	1
2FGLJ0024.5+0346	J002445.21+034903.7	BZQJ0024+0349	0.98(0.05)	2.96(0.09)	1.84(0.38)	0.545	-	-	-
2FGLJ0029.2-7043	J002841.53-704515.8	BZBJ0028-7045	1.0 (0.03)	2.6 (0.03)	2.15(0.07)	?	UND	C	3
2FGLJ0030.2-4223	J003017.48-422446.3	BZQJ0030-4224	1.17(0.03)	2.72(0.04)	2.14(0.1)	0.495	-	-	-
2FGLJ0033.5-1921	J003334.36-192132.9	BZBJ0033-1921	0.79(0.03)	2.14(0.04)	1.75(0.13)	0.61	BZB	B	0
2FGLJ0035.2+1515	J003514.71+151504.2	BZBJ0035+1515	0.77(0.03)	2.19(0.06)	1.92(0.23)	?	BZB	C	0
2FGLJ0037.8+1238	J003750.87+123819.9	BZBJ0037+1238	0.61(0.03)	2.13(0.04)	1.85(0.14)	?	BZB	B	1
2FGLJ0038.1+0015	J003808.49+001336.6	BZBJ0038+0013	0.95(0.05)	2.74(0.11)	2.38(0.31)	?	-	-	-
2FGLJ0038.3-2457	J003814.72-245902.2	BZQJ0038-2459	1.09(0.04)	3.18(0.05)	2.47(0.09)	1.196	BZQ	C	0
2FGLJ0043.7+3426	J004348.88+342625.9	BZQJ0043+3426	0.89(0.06)	2.89(0.11)	2.57(0.29)	0.966	-	-	-
2FGLJ0045.3+2127	J004519.28+212740.1	BZBJ0045+2127	0.72(0.03)	2.1 (0.05)	1.86(0.17)	?	BZB	C	1
2FGLJ0046.7-8416	J004426.56-842239.9	BZQJ0044-8422	1.03(0.04)	2.81(0.04)	2.49(0.08)	1.032	UND	C	3
2FGLJ0047.9+2232	J004802.60+223524.3	BZQJ0048+2235	1.02(0.05)	2.64(0.13)	2.35(0.42)	1.161	-	-	-
2FGLJ0049.7-5738	J004959.50-573826.7	BZQJ0049-5738	1.01(0.04)	2.81(0.04)	2.41(0.1)	1.797	UND	C	1
2FGLJ0050.1-0452	J005021.52-045220.3	BZQJ0050-0452	1.13(0.05)	2.82(0.1)	2.18(0.3)	0.92	-	-	-
2FGLJ0050.2+0234	J004943.22+023703.9	BZBJ0049+0237	1.03(0.04)	2.9(0.06)	2.6 (0.13)	?	BZQ	C	0
2FGLJ0050.6-0929	J005041.30-092904.9	BZBJ0050-0929	0.98(0.04)	2.6(0.05)	2.33(0.13)	?	UND	C	0
2FGLJ0051.0-0648	J005108.20-065001.9	BZQJ0051-0650	1.13(0.06)	3.16(0.11)	2.28(0.35)	1.975	-	-	-
2FGLJ0057.9-3236	J005802.21-323420.6	BZBJ0058-3234	1.01(0.03)	2.64(0.03)	2.23(0.07)	?	UND	B	0
2FGLJ0102.3+4216	J010227.15+421419.0	BZQJ0102+4214	1.05(0.03)	2.84(0.04)	2.42(0.09)	0.874	UND	C	1
2FGLJ0105.0-2411	J010458.18-241628.2	BZQJ0104-2416	1.2(0.05)	2.96(0.07)	2.81(0.14)	1.747	BZQ	C	3
2FGLJ0108.6+0135	J010838.76+013500.5	BZQJ0108+0135	1.15(0.04)	3.21(0.04)	2.64(0.06)	2.099	BZQ	B	0
2FGLJ0109.0+1817	J010908.17+181607.7	BZBJ0109+1816	0.81(0.03)	2.27(0.05)	1.99(0.15)	0.145	BZB	B	0
2FGLJ0112.1+2245	J011205.81+224438.9	BZBJ0112+2244	0.94(0.03)	2.46(0.02)	2.04(0.03)	?	BZB	A	0
2FGLJ0112.8+3208	J011250.33+320817.3	BZQJ0112+3208	1.04(0.03)	2.81(0.03)	2.36(0.04)	0.603	UND	B	0
2FGLJ0113.7+4948	J011327.00+494824.0	BZQJ0113+4948	1.09(0.03)	2.89(0.03)	2.37(0.05)	0.389	UND	C	0
2FGLJ0115.4+0358	J011540.50+035643.4	BZBJ0115+0356	0.94(0.03)	2.31(0.05)	2.0 (0.17)	?	BZB	C	1
2FGLJ0115.7+2518	J011546.14+251953.5	BZBJ0115+2519	0.68(0.04)	2.13(0.06)	2.19(0.23)	?	BZB	C	1
2FGLJ0116.0-1134	J011612.52-113615.3	BZQJ0116-1136	1.12(0.03)	2.79(0.03)	2.41(0.05)	0.67	UND	C	1
2FGLJ0118.8-2142	J011857.25-214129.9	BZQJ0118-2141	1.08(0.03)	2.9(0.04)	2.28(0.07)	1.165	UND	B	0
2FGLJ0120.4-2700	J012031.65-270124.5	BZBJ0120-2701	0.93(0.03)	2.59(0.03)	2.11(0.04)	?	BZB	A	0
2FGLJ0124.5-0621	J012450.46-062500.7	BZBJ0124-0625	1.14(0.04)	2.66(0.08)	2.05(0.29)	?	-	-	-
2FGLJ0132.8-1654	J013243.47-165448.4	BZQJ0132-1654	1.11(0.03)	2.89(0.03)	2.35(0.04)	1.02	UND	C	0
2FGLJ0136.5+3905	J013632.59+390559.2	BZBJ0136+3905	0.78(0.03)	2.1(0.03)	1.73(0.07)	?	BZB	B	0
2FGLJ0136.9+4751	J013658.58+475129.2	BZQJ0136+4751	1.07(0.03)	3.12(0.03)	2.47(0.03)	0.859	BZQ	A	0
2FGLJ0137.6-2430	J013738.34-243053.8	BZQJ0137-2430	1.16(0.03)	2.95(0.03)	2.61(0.04)	0.835	BZQ	A	0
2FGLJ0141.5-0928	J014125.81-092843.6	BZBJ0141-0928	1.02(0.03)	2.78(0.03)	2.33(0.04)	0.73?	UND	B	0
2FGLJ0145.1-2732	J014503.38-273334.1	BZQJ0145-2733	1.21(0.03)	3.15(0.03)	2.59(0.06)	1.148	BZQ	B	1
2FGLJ0152.6+0148	J015239.60+014717.4	BZBJ0152+0147	0.38(0.03)	1.71(0.04)	1.68(0.18)	0.08	-	-	-
2FGLJ0153.9+0823	J015402.76+082351.2	BZBJ0154+0823	0.88(0.03)	2.41(0.03)	2.15(0.06)	?	BZB	B	0
2FGLJ0154.9+4434	J015454.46+443337.9	BZBJ0154+4433	0.88(0.04)	2.26(0.06)	2.07(0.21)	?	BZB	C	0
2FGLJ0158.0-4609	J015751.11-461423.2	BZQJ0157-4614	1.04(0.09)	3.09(0.18)	2.48(0.51)	2.287	-	-	-
2FGLJ0158.3-3931	J015838.09-393203.7	BZBJ0158-3932	0.9 (0.03)	2.39(0.04)	1.99(0.09)	?	BZB	B	0
2FGLJ0159.5+1046	J015934.38+104705.8	BZBJ0159+1047	0.74(0.03)	2.16(0.05)	2.07(0.18)	?	BZB	C	0
2FGLJ0159.6-2741	J015943.34-274038.0	BZBJ0159-2740	0.85(0.03)	2.38(0.04)	1.93(0.13)	?	BZB	B	0
2FGLJ0203.6+7235	J020333.55+723253.0	BZBJ0203+7232	0.61(0.03)	2.28(0.03)	2.21(0.05)	?	-	-	-
2FGLJ0205.3-1657	J020457.66-170119.8	BZQJ0204-1701	1.09(0.04)	3.01(0.05)	2.4(0.12)	1.74	BZQ	C	4
2FGLJ0205.4+3211	J020504.92+321230.2	BZQJ0205+3212	1.56(0.04)	3.24(0.05)	2.24(0.13)	1.466	-	-	-
2FGLJ0206.5-1149	J020626.08-115039.7	BZQJ0206-1150	1.1 (0.03)	2.7 (0.04)	2.47(0.08)	1.663	UND	C	0
2FGLJ0209.5-5229	J020921.60-522922.7	BZBJ0209-5229	0.6 (0.03)	1.96(0.05)	1.77(0.1)	?	BZB	C	0
2FGLJ0211.2+1050	J021113.16+105134.8	BZBJ0211+1051	0.95(0.03)	2.49(0.02)	2.11(0.03)	?	BZB	A	0
2FGLJ0213.1+2245	J021252.81+224452.2	BZBJ0212+2244	0.54(0.03)	2.2 (0.06)	1.99(0.24)	0.459	BZB	C	0
2FGLJ0217.4+0836	J021717.11+083704.1	BZBJ0217+0837	0.84(0.03)	2.52(0.03)	2.11(0.04)	?	BZB	A	0
2FGLJ0217.5-0813	J021702.65-082052.2	BZQJ0217-0820	1.05(0.04)	3.02(0.04)	2.53(0.08)	0.607	BZQ	B	0
2FGLJ0217.9+0143	J021748.93+014449.9	BZQJ0217+0144	1.12(0.03)	2.94(0.03)	2.46(0.03)	1.715	BZQ	A	0
2FGLJ0219.1-1725	J021905.49-172512.9	BZBJ0219-1725	0.45(0.04)	1.72(0.11)	2.24(0.38)	0.128	-	-	-
2FGLJ0222.0-1615	J022200.71-161516.4	BZQJ0222-1615	1.12(0.03)	2.77(0.04)	2.51(0.1)	0.698	BZQ	C	1
2FGLJ0222.6+4302	J022239.60+430207.8	BZBJ0222+4302	0.83(0.03)	2.23(0.03)	1.94(0.03)	0.444?	BZB	A	0
2FGLJ0229.3-3644	J022928.42-364356.7	BZQJ0229-3643	1.13(0.05)	3.06(0.07)	2.28(0.19)	2.115	BZQ	C	2
2FGLJ0230.8+4031	J023045.70+403253.1	BZQJ0230+4032	1.16(0.04)	2.86(0.05)	2.31(0.12)	1.019	-	-	-

Continued on next page

TABLE 8 – *Continued from previous page*

2FGL name	WISE name	ROMA-BZCAT name	[3.4]-[4.6] mag	[4.6]-[12] mag	[12]-[22] mag	z	type	class	N <sub>BR</sub>
2FGLJ0237.1-6136	J023653.23-613615.2	BZQJ0236-6136	0.99(0.03)	2.79(0.02)	2.25(0.03)	0.465	UND	A	0
2FGLJ0237.8+2846	J023752.39+284808.9	BZQJ0237+2848	1.1 (0.03)	2.9 (0.03)	2.4 (0.05)	1.213	BZQ	B	0
2FGLJ0238.6-3117	J023832.47-311657.9	BZBJ0238-3116	0.64(0.03)	1.91(0.04)	1.73(0.19)	?	BZB	C	0
2FGLJ0238.7+1637	J023838.92+163659.4	BZBJ0238+1636	1.1 (0.03)	2.99(0.03)	2.43(0.04)	0.94	BZQ	A	0
2FGLJ0242.9+7118	J024330.88+712017.8	BZBJ0243+7120	0.9 (0.03)	2.36(0.04)	2.36(0.09)	?	BZB	C	0
2FGLJ0245.1+2406	J024516.83+240535.0	BZQJ0245+2405	1.04(0.09)	3.09(0.1)	2.55(0.47)	2.243	-	-	-
2FGLJ0245.9-4652	J024600.09-465117.1	BZQJ0246-4651	1.08(0.03)	2.93(0.03)	2.46(0.06)	1.385	BZQ	B	0
2FGLJ0252.7-2218	J025247.94-221925.3	BZQJ0252-2219	1.12(0.04)	3.05(0.04)	2.56(0.09)	1.427	BZQ	B	0
2FGLJ0257.7-1213	J025741.00-121201.3	BZQJ0257-1212	1.21(0.04)	2.74(0.07)	1.85(0.28)	1.391	-	-	-
2FGLJ0259.5+0740	J025927.06+074739.6	BZQJ0259+0747	1.01(0.04)	2.92(0.06)	2.48(0.14)	0.893	-	-	-
2FGLJ0302.7-7919	J030320.89-791456.5	BZQJ0303-7914	1.2 (0.04)	3.01(0.05)	2.52(0.1)	1.115	BZQ	C	1
2FGLJ0303.4-2407	J030326.49-240711.4	BZBJ0303-2407	0.86(0.03)	2.27(0.03)	1.98(0.04)	0.267	BZB	A	0
2FGLJ0303.5-6209	J030350.61-621125.5	BZQJ0303-6211	1.22(0.03)	2.97(0.03)	2.35(0.05)	1.351	BZQ	B	0
2FGLJ0309.1+1027	J030903.61+102916.3	BZQJ0309+1029	1.06(0.03)	2.92(0.03)	2.4 (0.05)	0.863	BZQ	C	0
2FGLJ0310.0-6058	J030956.07-605838.9	BZQJ0309-6058	1.1 (0.03)	3.0 (0.03)	2.46(0.05)	1.48	BZQ	B	0
2FGLJ0310.7+3813	J031049.87+381453.9	BZQJ0310+3814	1.11(0.04)	3.0 (0.06)	2.5 (0.13)	0.816?	BZQ	C	0
2FGLJ0312.6+0132	J031243.60+013317.6	BZQJ0312+0133	1.06(0.04)	2.8 (0.05)	2.58(0.1)	0.664	BZQ	C	0
2FGLJ0314.2-5106	J031425.69-510431.5	BZBJ0314-5104	1.02(0.04)	2.67(0.04)	2.12(0.12)	?	UND	C	0
2FGLJ0315.8-2611	J031614.93-260757.2	BZBJ0316-2607	0.75(0.03)	2.14(0.04)	1.78(0.18)	0.443	BZB	C	1
2FGLJ0316.1+0904	J031612.72+090443.3	BZBJ0316+0904	0.76(0.03)	2.19(0.03)	1.95(0.07)	?	BZB	B	0
2FGLJ0322.0+2336	J032159.96+233611.2	BZBJ0321+2326	0.75(0.03)	2.02(0.06)	2.31(0.15)	?	-	-	-
2FGLJ0325.6-1650	J032541.09-164616.8	BZBJ0325-1646	0.7 (0.04)	2.01(0.07)	2.2 (0.23)	0.291	BZB	C	2
2FGLJ0326.1+0224	J032613.94+022514.7	BZBJ0326+0225	0.56(0.04)	2.0 (0.08)	1.75(0.39)	0.147	BZB	C	1
2FGLJ0326.1+2226	J032536.80+222400.4	BZQJ0325+2224	1.22(0.04)	3.2 (0.04)	2.47(0.09)	2.066	BZQ	B	0
2FGLJ0334.2-4008	J033413.64-400825.4	BZBJ0334-4008	1.07(0.03)	2.88(0.02)	2.34(0.03)	?	UND	A	0
2FGLJ0334.3-3728	J033415.41-372543.1	BZBJ0334-3725	0.95(0.03)	2.62(0.03)	2.18(0.03)	?	UND	C	0
2FGLJ0339.4-0144	J033930.93-014635.7	BZQJ0339-0146	1.14(0.03)	2.91(0.03)	2.45(0.05)	0.85	BZQ	B	1
2FGLJ0340.6-2113	J034035.60-211931.0	BZBJ0340-2119	0.98(0.03)	2.75(0.03)	2.22(0.05)	0.223	UND	B	0
2FGLJ0342.4+3859	J034216.26+385906.2	BZQJ0342+3859	1.03(0.04)	2.57(0.06)	2.2 (0.1)	0.945	UND	C	0
2FGLJ0348.6-2750	J034838.13-274913.5	BZQJ0348-2749	1.09(0.04)	3.04(0.05)	2.37(0.12)	0.991	BZQ	C	0
2FGLJ0350.0-2104	J034957.81-210247.6	BZQJ0349-2102	1.11(0.08)	3.56(0.11)	2.28(0.38)	2.944	-	-	-
2FGLJ0354.1+8010	J035446.07+800928.8	BZBJ0354+8009	0.98(0.04)	2.72(0.08)	2.59(0.18)	?	-	-	-
2FGLJ0357.0-4950	J035700.17-495548.6	BZBJ0357-4955	0.93(0.03)	2.54(0.03)	2.01(0.05)	?	BZB	B	0
2FGLJ0402.0-2616	J040200.77-261539.3	BZBJ0402-2615	1.01(0.04)	2.7 (0.04)	2.13(0.12)	?	UND	C	0
2FGLJ0403.9-3604	J040353.75-360501.9	BZQJ0403-3605	1.2 (0.03)	3.24(0.03)	2.52(0.03)	1.417	BZQ	A	0
2FGLJ0405.8-1309	J040533.99-130813.6	BZQJ0405-1308	1.09(0.03)	2.45(0.03)	2.12(0.06)	0.571	UND	C	2
2FGLJ0407.7+0740	J040729.07+074208.1	BZBJ0407+0742	0.98(0.04)	2.94(0.07)	2.52(0.15)	1.133?	-	-	-
2FGLJ0413.5-5332	J041313.41-533200.4	BZQJ0413-5332	1.02(0.04)	3.02(0.07)	2.58(0.18)	1.027	BZQ	C	0
2FGLJ0416.7-1849	J041636.53-185108.3	BZQJ0416-1851	1.26(0.05)	3.14(0.07)	2.64(0.16)	1.421	BZQ	C	1
2FGLJ0416.8+0105	J041652.48+010523.9	BZBJ0416+0105	0.66(0.04)	1.83(0.07)	1.88(0.27)	0.287	BZB	C	1
2FGLJ0422.1-0645	J042210.78-064345.3	BZQJ0422-0643	0.96(0.03)	2.8 (0.03)	2.31(0.06)	0.242	UND	B	0
2FGLJ0423.2-0120	J042315.79-012032.9	BZQJ0423-0120	1.1 (0.03)	3.06(0.03)	2.42(0.02)	0.916	BZQ	A	0
2FGLJ0424.7+0034	J042446.83+003606.3	BZBJ0424+0036	0.98(0.03)	2.62(0.03)	2.14(0.03)	?	UND	C	0
2FGLJ0428.6-3756	J042840.41-375619.6	BZBJ0428-3756	1.02(0.03)	2.65(0.02)	2.27(0.03)	1.03?	UND	A	0
2FGLJ0430.4-2507	J043016.01-250738.9	BZBJ0430-2507	0.83(0.04)	2.49(0.06)	2.08(0.21)	?	BZB	C	2
2FGLJ0434.1-2014	J043407.91-201517.1	BZBJ0434-2015	0.94(0.04)	2.58(0.05)	2.48(0.11)	?	UND	C	6
2FGLJ0439.0-1252	J043835.01-125103.3	BZQJ0438-1251	1.08(0.04)	2.97(0.06)	2.21(0.19)	1.276	UND	C	2
2FGLJ0440.9+2749	J044050.36+275046.9	BZBJ0440+2750	0.65(0.03)	1.98(0.07)	2.12(0.22)	?	BZB	C	0
2FGLJ0442.7-0017	J044238.65-001743.2	BZQJ0442-0017	1.04(0.03)	2.89(0.04)	2.34(0.06)	0.844	UND	B	0
2FGLJ0448.5-1633	J044837.61-163243.1	BZBJ0448-1632	0.8 (0.04)	2.08(0.09)	2.27(0.29)	?	-	-	-
2FGLJ0448.6-2118	J044817.37-210944.7	BZQJ0448-2109	0.96(0.05)	2.89(0.08)	2.21(0.26)	1.971	UND	C	6
2FGLJ0449.4-4350	J044924.69-435008.9	BZBJ0449-4350	0.83(0.03)	2.27(0.02)	1.91(0.03)	0.205?	BZB	A	0
2FGLJ0453.1-2807	J045314.64-280737.2	BZQJ0453-2807	1.04(0.04)	3.23(0.04)	2.57(0.06)	2.564	BZQ	B	0
2FGLJ0456.5-3132	J045636.68-313612.5	BZQJ0456-3136	1.06(0.04)	2.92(0.06)	2.57(0.13)	0.865	BZQ	C	3
2FGLJ0457.0-2325	J045703.18-232452.0	BZQJ0457-2324	1.11(0.03)	2.95(0.03)	2.39(0.03)	1.003	BZQ	A	0
2FGLJ0501.2-0155	J050112.80-015914.2	BZQJ0501-0159	1.13(0.03)	3.09(0.04)	2.49(0.06)	2.291	BZQ	B	1
2FGLJ0502.5+0607	J050215.43+060907.5	BZQJ0502+0609	1.11(0.05)	3.08(0.07)	2.47(0.16)	1.106	BZQ	C	1
2FGLJ0505.5+0501	J050523.18+045942.8	BZQJ0505+0459	1.17(0.03)	3.1 (0.03)	2.51(0.04)	0.954	BZQ	B	1
2FGLJ0507.5-6102	J050754.64-610443.2	BZQJ0507-6104	1.1 (0.03)	2.85(0.04)	2.51(0.09)	1.088	BZQ	B	0
2FGLJ0508.0+6737	J050756.16+673724.3	BZBJ0507+6737	0.69(0.03)	1.92(0.05)	1.53(0.22)	0.416?	BZB	C	0
2FGLJ0509.2+1013	J050927.44+101144.6	BZQJ0509+1011	0.95(0.05)	2.71(0.1)	2.38(0.31)	0.621	UND	C	0
2FGLJ0509.4+0542	J050925.96+054135.3	BZBJ0509+0541	0.9 (0.03)	2.44(0.02)	2.07(0.03)	?	BZB	A	0
2FGLJ0515.9+1528	J051547.35+152716.5	BZBJ0515+1527	0.82(0.03)	2.35(0.04)	1.93(0.11)	?	BZB	B	0
2FGLJ0516.5-4601	J051545.23-455643.3	BZQJ0515-4556	0.95(0.03)	2.8 (0.03)	2.43(0.04)	0.194	UND	B	2
2FGLJ0526.1-4829	J052616.66-483036.8	BZQJ0526-4830	1.14(0.03)	3.0 (0.03)	2.33(0.07)	1.299	BZQ	B	0
2FGLJ0530.8+1333	J053056.40+133155.2	BZQJ0530+1331	0.89(0.06)	2.91(0.12)	2.74(0.24)	2.07	-	-	-
2FGLJ0531.8-8324	J053338.36-832435.8	BZQJ0533-8324	1.06(0.04)	3.01(0.04)	2.27(0.1)	0.774	UND	C	1
2FGLJ0532.7+0733	J053239.00+073243.3	BZQJ0532+0732	1.12(0.04)	3.1 (0.04)	2.53(0.08)	1.254	BZQ	B	0
2FGLJ0536.2-3348	J053629.06-334302.5	BZBJ0536-3343	0.68(0.03)	2.04(0.05)	2.23(0.16)	?	-	-	-
2FGLJ0538.8-4405	J053850.35-440509.0	BZBJ0538-4405	1.07(0.03)	2.75(0.02)	2.24(0.02)	0.892	UND	A	0
2FGLJ0539.3-2841	J053954.26-283956.2	BZQJ0539-2839	0.97(0.09)	3.27(0.15)	2.76(0.37)	3.104	-	-	-
2FGLJ0540.4-5415	J054045.83-541822.1	BZQJ0540-5418	1.08(0.03)	2.81(0.03)	2.3(0.07)	1.185	UND	B	0
2FGLJ0543.9-5532	J054357.21-553207.5	BZBJ0543-5532	0.68(0.03)	1.99(0.04)	1.72(0.16)	?	BZB	B	0
2FGLJ0558.7-7501	J055846.03-745905.2	BZBJ0558-7459	0.97(0.03)	2.57(0.03)	2.13(0.04)	?	BZB	C	2
2FGLJ0607.4+4739	J060723.24+473947.0	BZBJ0607+4739	0.88(0.03)	2.4 (0.03)	2.02(0.04)	?	BZB	A	0

*Continued on next page*



TABLE 8 – *Continued from previous page*

2FGL name	WISE name	ROMA-BZCAT name	[3.4]-[4.6] mag	[4.6]-[12] mag	[12]-[22] mag	z	type	class	N <sub>BR</sub>
2FGLJ0608.0-0836	J060759.61-083451.6	BZQJ0607-0834	0.39(0.04)	1.88(0.06)	2.16(0.1)	0.872	-	-	-
2FGLJ0609.6-1847	J061017.88-184740.1	BZBJ0610-1847	1.04(0.03)	2.89(0.03)	2.38(0.06)	?	UND	B	1
2FGLJ0611.8-6059	J061030.31-605838.1	BZQJ0610-6058	1.27(0.08)	2.97(0.15)	2.79(0.35)	1.773	-	-	-
2FGLJ0612.8+4122	J061251.18+412237.4	BZBJ0612+4122	0.97(0.03)	2.6(0.03)	2.14(0.05)	?	UND	C	0
2FGLJ0616.9+5701	J061716.91+570116.5	BZBJ0617+5701	0.96(0.03)	2.57(0.03)	2.1(0.05)	?	BZB	B	0
2FGLJ0617.6-1716	J061733.42-171525.0	BZBJ0617-1715	0.18(0.03)	1.46(0.08)	2.14(0.27)	?	-	-	-
2FGLJ0625.2+4441	J062518.26+444001.6	BZBJ0625+4440	0.94(0.03)	2.62(0.04)	1.97(0.11)	?	BZB	B	0
2FGLJ0629.3-2001	J062923.76-195919.8	BZBJ0629-1959	1.09(0.03)	2.75(0.03)	2.31(0.05)	?	UND	B	0
2FGLJ0630.9-2406	J063059.51-240646.2	BZBJ0630-2406	0.85(0.03)	2.24(0.03)	1.93(0.07)	?	BZB	B	0
2FGLJ0635.5-7516	J063546.51-751616.9	BZQJ0635-7516	1.07(0.03)	2.8(0.02)	2.36(0.03)	0.653	UND	A	0
2FGLJ0650.7+2505	J065046.48+250259.6	BZBJ0650+2503	0.72(0.03)	2.08(0.04)	1.73(0.15)	0.203?	-	-	-
2FGLJ0654.5+5043	J065422.06+504223.7	BZQJ0654+5042	0.82(0.03)	2.69(0.04)	2.24(0.08)	1.253	BZB	B	0
2FGLJ0700.3-6611	J070031.24-661045.2	BZBJ0700-6610	0.9(0.03)	2.4(0.02)	2.02(0.03)	?	BZB	A	0
2FGLJ0701.7-4630	J070134.54-463436.7	BZQJ0701-4634	1.18(0.03)	3.1(0.03)	2.48(0.05)	0.822	BZQ	B	1
2FGLJ0710.5+5908	J071030.05+590820.5	BZBJ0710+5908	0.48(0.03)	1.78(0.06)	2.04(0.22)	0.125	-	-	-
2FGLJ0710.8+4733	J071046.30+473213.2	BZBJ0710+4732	0.19(0.03)	1.84(0.06)	2.3(0.17)	1.292??	-	-	-
2FGLJ0712.9+5032	J071243.68+503322.7	BZBJ0712+5033	1.04(0.03)	2.7(0.03)	2.25(0.05)	?	UND	B	0
2FGLJ0714.0+1933	J071355.67+193500.4	BZQJ0713+1935	0.99(0.03)	2.69(0.03)	2.26(0.05)	0.54	UND	B	0
2FGLJ0718.7-4320	J071843.63-431949.8	BZBJ0718-43.4	0.89(0.03)	2.23(0.04)	1.68(0.17)	?	-	-	-
2FGLJ0721.9+7120	J072153.44+712036.3	BZBJ0721+7120	0.98(0.03)	2.65(0.02)	2.11(0.02)	?	UND	C	0
2FGLJ0725.3+1426	J072516.80+142513.6	BZQJ0725+1425	1.09(0.04)	2.83(0.04)	2.52(0.09)	1.038	BZQ	B	0
2FGLJ0727.0-4726	J072626.23-472853.4	BZQJ0726-4728	1.09(0.04)	2.97(0.05)	2.28(0.16)	1.686	BZQ	C	0
2FGLJ0729.9+3304	J073026.06+330722.9	BZBJ0730+3307	0.84(0.03)	2.26(0.05)	1.75(0.19)	0.112	-	-	-
2FGLJ0733.9+5023	J073352.51+502209.2	BZQJ0733+5022	1.04(0.04)	2.72(0.06)	2.64(0.12)	0.72	-	-	-
2FGLJ0738.0+1742	J073807.39+174219.0	BZBJ0738+1742	0.94(0.03)	2.6(0.03)	2.03(0.04)	0.424	BZB	B	0
2FGLJ0739.2+0138	J073918.03+013704.6	BZQJ0739+0137	1.0(0.03)	2.72(0.03)	2.26(0.03)	0.191	UND	A	0
2FGLJ0746.6+2549	J074625.85+254902.4	BZQJ0746+2549	1.15(0.12)	3.63(0.1)	2.54(0.48)	2.979	-	-	-
2FGLJ0747.7+4501	J074906.50+451033.9	BZQJ0749+4510	1.01(0.03)	2.84(0.03)	2.62(0.04)	0.192	BZQ	A	0
2FGLJ0750.6+1230	J075052.04+123104.8	BZQJ0750+1231	1.08(0.03)	2.82(0.03)	2.46(0.05)	0.889	UND	C	0
2FGLJ0753.0+5352	J075301.38+535259.8	BZBJ0753+5352	1.02(0.04)	2.92(0.05)	2.46(0.11)	?	-	-	-
2FGLJ0754.8+4824	J075445.66+482350.7	BZBJ0754+4823	1.04(0.03)	2.73(0.03)	2.3(0.04)	?	UND	B	0
2FGLJ0757.1+0957	J075706.64+095634.8	BZBJ0757+0956	1.06(0.03)	2.83(0.03)	2.45(0.04)	0.266	BZQ	C	0
2FGLJ0801.5+4401	J080108.28+440110.2	BZBJ0801+4401	1.1(0.05)	2.75(0.07)	2.17(0.25)	?	UND	C	3
2FGLJ0805.3+7535	J080526.63+753424.9	BZBJ0805+7534	0.54(0.03)	2.01(0.04)	1.81(0.17)	0.121	BZB	B	0
2FGLJ0805.5+6145	J080518.15+614424.0	BZQJ0805+6144	1.17(0.09)	3.39(0.13)	2.76(0.27)	3.033	-	-	-
2FGLJ0807.1-0543	J080709.61-054113.9	BZBJ0807-0541	0.96(0.03)	2.7(0.04)	2.21(0.09)	?	UND	B	0
2FGLJ0808.2-0750	J080815.53-075109.9	BZQJ0808-0751	0.99(0.03)	2.74(0.03)	2.31(0.03)	1.837	UND	A	0
2FGLJ0809.8+5218	J080949.19+521858.3	BZBJ0809+5218	0.68(0.03)	2.06(0.03)	1.84(0.1)	0.138	BZB	B	0
2FGLJ0811.1-7527	J081103.23-753027.9	BZBJ0811-7530	0.79(0.03)	2.29(0.03)	1.89(0.1)	?	-	-	-
2FGLJ0811.4+0149	J081126.71+014652.2	BZBJ0811+0146	1.09(0.04)	3.06(0.05)	2.56(0.11)	1.148	BZQ	C	1
2FGLJ0814.0-1006	J081411.69-101210.3	BZBJ0814-1012	0.83(0.03)	2.33(0.03)	1.97(0.08)	?	BZB	B	0
2FGLJ0814.7+6429	J081439.19+643122.0	BZBJ0814+6431	0.92(0.03)	2.48(0.03)	2.04(0.04)	?	BZB	A	0
2FGLJ0816.4-1311	J081627.20-131152.6	BZBJ0816-1311	0.77(0.04)	1.94(0.06)	1.78(0.24)	?	BZB	C	0
2FGLJ0816.5+5739	J081622.71+573909.2	BZBJ0816+5739	0.84(0.03)	2.35(0.04)	2.09(0.11)	?	BZB	B	0
2FGLJ0816.9+2049	J081649.78+205106.4	BZBJ0816+2051	0.92(0.04)	2.24(0.08)	1.67(0.42)	?	-	-	-
2FGLJ0817.9+3238	J081750.99+324340.7	BZBJ0817+3243	0.73(0.05)	2.31(0.13)	2.32(0.4)	?	-	-	-
2FGLJ0818.2-0935	J081749.75-093330.5	BZBJ0817-0933	1.02(0.03)	2.54(0.03)	2.32(0.06)	?	UND	-	-
2FGLJ0819.3+2750	J081918.85+274730.7	BZBJ0819+2747	1.04(0.04)	2.73(0.05)	2.54(0.09)	?	UND	C	1
2FGLJ0819.6-0803	J081917.58-075626.0	BZBJ0819-0756	0.51(0.05)	2.0(0.1)	3.61(0.28)	?	-	-	-
2FGLJ0824.7+3914	J082455.47+391641.9	BZQJ0824+3916	1.24(0.04)	3.12(0.05)	2.51(0.12)	1.216	BZQ	C	1
2FGLJ0824.9+5552	J082447.23+555242.8	BZQJ0824+5552	1.23(0.05)	2.99(0.07)	2.59(0.17)	1.417	BZQ	C	0
2FGLJ0825.9+0308	J082550.35+030924.4	BZBJ0825+0309	1.0(0.03)	2.72(0.03)	2.3(0.04)	0.506	UND	B	1
2FGLJ0830.5+2407	J083052.09+241059.8	BZQJ0830+2410	1.19(0.03)	3.11(0.04)	2.37(0.07)	0.939?	BZQ	B	0
2FGLJ0831.9+0429	J083148.88+042939.0	BZBJ0831+0429	0.98(0.03)	2.6(0.03)	2.16(0.03)	0.174	UND	C	0
2FGLJ0834.3+4221	J083353.88+422401.9	BZQJ0833+4224	1.03(0.03)	2.75(0.03)	2.28(0.05)	0.249	UND	B	0
2FGLJ0834.3+4400	J083458.19+440338.2	BZBJ0834+4403	0.92(0.03)	2.56(0.04)	2.16(0.1)	?	-	-	-
2FGLJ0839.6+0059	J083949.61+010426.9	BZQJ0839+0104	1.2(0.06)	3.08(0.1)	2.32(0.3)	1.123	BZQ	C	0
2FGLJ0839.7+3541	J083943.36+354001.5	BZBJ0839+3540	0.88(0.04)	2.29(0.07)	2.19(0.23)	?	BZB	C	1
2FGLJ0841.6+7052	J084124.35+705342.2	BZQJ0841+7053	1.12(0.04)	3.39(0.04)	2.55(0.07)	2.218	BZQ	B	0
2FGLJ0843.9+5312	J084411.70+531250.7	BZBJ0844+5312	0.84(0.04)	2.48(0.06)	2.02(0.26)	?	BZB	C	0
2FGLJ0847.2+1134	J084712.93+113350.2	BZBJ0847+1133	0.61(0.04)	1.81(0.12)	2.08(0.54)	0.199	-	-	-
2FGLJ0848.1-0703	J084756.73-070316.8	BZBJ0847-0703	1.02(0.03)	2.75(0.03)	2.24(0.04)	?	UND	A	0
2FGLJ0849.0+0455	J084932.55+045507.8	BZBJ0849+0455	0.82(0.04)	2.52(0.08)	2.24(0.27)	?	BZB	C	1
2FGLJ0849.2+6606	J084854.60+660609.3	BZBJ0848+6606	0.73(0.04)	2.15(0.09)	1.63(0.53)	?	-	-	-
2FGLJ0849.8+4852	J085000.35+485458.8	BZBJ0850+4854	0.97(0.03)	2.65(0.03)	2.19(0.03)	?	UND	A	0
2FGLJ0850.2-1212	J085009.64-121335.3	BZQJ0850-1213	1.05(0.03)	2.79(0.03)	2.27(0.03)	0.566	UND	A	0
2FGLJ0854.8+2005	J085448.87+200630.7	BZBJ0854+2006	1.04(0.03)	2.72(0.03)	2.28(0.04)	0.306	UND	A	0
2FGLJ0856.3+2058	J085639.74+205743.4	BZBJ0856+2057	0.9(0.04)	2.63(0.07)	2.07(0.31)	0.18?	-	-	-
2FGLJ0856.6-1105	J085641.80-110514.4	BZBJ0856-1105	0.95(0.03)	2.58(0.03)	2.08(0.06)	?	BZB	B	0
2FGLJ0902.4+2050	J090226.91+205046.5	BZBJ0902+2050	0.89(0.03)	2.41(0.03)	2.04(0.08)	?	BZB	B	0
2FGLJ0903.4+4651	J090303.99+465104.2	BZQJ0903+4651	1.19(0.04)	3.14(0.06)	2.31(0.15)	1.462	BZQ	C	1
2FGLJ0905.6+1357	J090534.98+135806.4	BZBJ0905+1358	0.85(0.03)	2.29(0.04)	2.08(0.1)	?	BZB	B	1
2FGLJ0909.1+0121	J090910.08+012135.6	BZQJ0909+0121	1.18(0.03)	2.91(0.03)	2.4(0.06)	1.024	BZQ	B	0
2FGLJ0909.2+2308	J090900.63+231113.0	BZBJ0909+2311	0.75(0.04)	2.1(0.08)	2.19(0.26)	0.223	BZB	C	0
2FGLJ0909.7-0229	J090944.90-023129.2	BZQJ0909-0231	0.83(0.04)	2.42(0.09)	2.54(0.21)	0.957	-	-	-

*Continued on next page*

TABLE 8 – *Continued from previous page*

2FGL name	WISE name	ROMA-BZCAT name	[3.4]-[4.6] mag	[4.6]-[12] mag	[12]-[22] mag	z	type	class	N <sub>BR</sub>
2FGLJ0910.6+3329	J091037.04+332924.5	BZBJ0910+3329	0.87(0.03)	2.38(0.03)	1.91(0.09)	?	BZB	B	0
2FGLJ0912.1+4126	J091211.61+412609.4	BZQJ0912+4126	1.21(0.06)	2.96(0.12)	2.88(0.22)	2.563	-	-	-
2FGLJ0912.9-2102	J091300.22-210321.0	BZBJ0913-2103	0.6 (0.03)	2.04(0.04)	2.13(0.11)	0.198	BZB	C	0
2FGLJ0915.8+2932	J091552.40+293324.0	BZBJ0915+2933	0.76(0.03)	2.24(0.04)	1.89(0.1)	?	BZB	B	0
2FGLJ0917.0+3900	J091648.89+385428.2	BZQJ0916+3854	1.1 (0.05)	2.89(0.09)	2.3 (0.25)	1.267	-	-	-
2FGLJ0920.9+4441	J092058.46+444154.1	BZQJ0920+4441	1.21(0.04)	3.28(0.04)	2.54(0.07)	2.19	BZQ	B	0
2FGLJ0921.9+6216	J092136.24+621552.3	BZQJ0921+6215	1.14(0.04)	3.19(0.05)	2.62(0.09)	1.446	BZQ	C	0
2FGLJ0924.0+2819	J092351.52+281525.1	BZQJ0923+2815	1.07(0.04)	3.1 (0.06)	2.22(0.17)	0.744	-	-	-
2FGLJ0927.9-2041	J092751.82-203451.2	BZQJ0927-2034	1.03(0.03)	2.7 (0.03)	2.26(0.05)	0.348	UND	B	1
2FGLJ0929.5+5009	J092915.43+501336.1	BZBJ0929+5013	1.0 (0.03)	2.88(0.04)	2.22(0.08)	?	UND	B	0
2FGLJ0934.7+3932	J093406.65+392632.2	BZBJ0934+3926	1.18(0.07)	2.87(0.13)	2.89(0.26)	?	-	-	-
2FGLJ0937.6+5009	J093712.32+500852.1	BZQJ0937+5008	1.15(0.03)	3.06(0.04)	2.53(0.07)	0.276	BZQ	B	0
2FGLJ0945.9+5751	J094542.21+575747.6	BZBJ0945+5757	0.76(0.03)	2.35(0.03)	1.98(0.08)	0.229	BZB	B	0
2FGLJ0946.5+1015	J094635.06+101706.1	BZQJ0946+1017	1.09(0.05)	2.7 (0.08)	1.97(0.34)	1.007	-	-	-
2FGLJ0948.8+4040	J094855.34+403944.6	BZQJ0948+4039	1.28(0.04)	3.02(0.06)	1.97(0.21)	1.249	UND	-	-
2FGLJ0950.1+4554	J095011.82+455320.1	BZBJ0950+4553	0.9 (0.04)	2.48(0.06)	2.25(0.17)	0.399	BZB	C	2
2FGLJ0953.1-0839	J095302.71-084018.2	BZBJ0953-0840	0.83(0.03)	2.34(0.04)	2.03(0.1)	?	BZB	B	0
2FGLJ0956.9+2516	J095649.88+251516.1	BZQJ0956+2515	1.13(0.03)	2.96(0.03)	2.46(0.06)	0.708	BZQ	B	0
2FGLJ0957.6-1350	J095718.18-135001.2	BZQJ0957-1350	1.16(0.05)	2.83(0.08)	2.39(0.24)	1.323	BZQ	C	1
2FGLJ0957.7+5522	J095738.17+552257.8	BZQJ0957+5522	1.04(0.03)	2.89(0.03)	2.36(0.06)	0.899	UND	B	0
2FGLJ0958.6+6533	J095847.23+653354.9	BZBJ0958+6533	1.01(0.03)	2.75(0.03)	2.22(0.03)	0.367	UND	A	0
2FGLJ1001.0+2913	J100110.20+291137.6	BZBJ1001+2911	1.04(0.03)	2.76(0.03)	2.26(0.06)	0.558	UND	B	0
2FGLJ1007.1-2157	J100646.41-215920.4	BZQJ1006-2159	0.99(0.03)	2.48(0.03)	2.28(0.06)	0.33	UND	C	0
2FGLJ1007.7+0621	J100800.81+062121.2	BZBJ1008+0621	0.99(0.03)	2.66(0.03)	2.18(0.04)	?	UND	B	0
2FGLJ1009.7-3123	J101015.98-311908.3	BZBJ1010-3119	0.46(0.03)	1.72(0.07)	1.88(0.31)	0.143	-	-	-
2FGLJ1010.8-0158	J101051.67-020019.5	BZQJ1010-0200	1.1 (0.05)	2.93(0.11)	2.39(0.26)	0.887	-	-	-
2FGLJ1012.1+0631	J101213.35+063057.2	BZBJ1012+0630	0.96(0.04)	2.68(0.04)	2.02(0.15)	0.518?	BZB	C	0
2FGLJ1012.6+2440	J101241.39+243923.2	BZQJ1012+2439	1.16(0.09)	2.71(0.25)	2.98(0.5)	1.805	-	-	-
2FGLJ1014.1+2306	J101447.08+230116.7	BZQJ1014+2301	1.07(0.04)	2.75(0.04)	2.56(0.08)	0.566	UND	C	5
2FGLJ1015.1+4925	J101504.13+492600.8	BZBJ1015+4926	0.8 (0.03)	2.21(0.03)	2.06(0.05)	0.212	BZB	B	0
2FGLJ1016.0+0513	J101603.13+051302.2	BZQJ1016+0513	1.12(0.06)	3.19(0.11)	2.64(0.23)	1.714	BZQ	C	0
2FGLJ1017.0+3531	J101810.98+354239.6	BZQJ1018+3542	1.33(0.05)	2.8 (0.07)	2.33(0.1)	1.226	-	-	-
2FGLJ1018.3-3119	J101828.76-312353.8	BZQJ1018-3123	1.15(0.03)	2.87(0.04)	2.46(0.09)	0.794	BZQ	B	1
2FGLJ1019.0+5915	J101858.54+591127.9	BZBJ1018+5911	0.72(0.04)	2.42(0.06)	2.23(0.18)	?	BZB	C	2
2FGLJ1019.8+6322	J101950.86+632001.7	BZBJ1019+6320	1.02(0.03)	2.69(0.03)	2.21(0.06)	?	UND	B	3
2FGLJ1023.1-0115	J102243.73-011302.2	BZBJ1022-0113	0.69(0.04)	1.88(0.13)	1.96(0.55)	?	-	-	-
2FGLJ1023.8-3248	J102400.42-323416.1	BZQJ1024-3234	1.15(0.04)	3.1 (0.06)	2.37(0.15)	1.568	-	-	-
2FGLJ1023.8-4335	J102356.20-433601.5	BZBJ1023-4336	0.76(0.03)	2.04(0.04)	1.79(0.17)	?	BZB	B	0
2FGLJ1026.3-8546	J102634.47-854314.2	BZBJ1026-8543	0.87(0.03)	2.32(0.03)	2.02(0.08)	?	BZB	B	0
2FGLJ1026.7-1749	J102658.57-174858.8	BZBJ1026-1748	0.64(0.03)	2.05(0.06)	1.8 (0.26)	0.114?	BZB	C	0
2FGLJ1032.6+3733	J103240.73+373826.8	BZBJ1032+3738	0.92(0.03)	2.46(0.05)	1.99(0.18)	?	BZB	C	2
2FGLJ1033.2+4117	J103303.70+411606.2	BZQJ1033+4116	1.23(0.03)	3.27(0.03)	2.59(0.04)	1.117	BZQ	A	0
2FGLJ1037.5-2820	J103742.46-282304.0	BZQJ1037-2823	1.07(0.04)	2.78(0.05)	2.43(0.12)	1.066	UND	C	0
2FGLJ1037.6+5712	J103744.30+571155.7	BZBJ1037+5711	0.91(0.03)	2.42(0.03)	1.93(0.09)	?	BZB	B	0
2FGLJ1040.7+0614	J104117.17+061017.0	BZQJ1041+0610	1.43(0.04)	3.21(0.04)	2.51(0.08)	1.264	-	-	-
2FGLJ1042.6+8053	J104423.03+805439.5	BZQJ1044+8054	1.09(0.03)	2.88(0.03)	2.36(0.04)	1.254	UND	C	4
2FGLJ1043.1+2404	J104309.04+240835.5	BZQJ1043+2408	0.96(0.04)	2.69(0.04)	2.33(0.09)	0.559	UND	B	0
2FGLJ1049.7+7240	J104747.51+723813.0	BZBJ1047+7238	0.85(0.03)	2.34(0.03)	2.01(0.08)	?	-	-	-
2FGLJ1051.8+0107	J105151.83+010311.5	BZBJ1051+0103	0.67(0.04)	2.01(0.14)	2.56(0.36)	0.265	-	-	-
2FGLJ1053.6+4928	J105344.13+492956.1	BZBJ1053+4929	0.41(0.03)	1.78(0.06)	1.37(0.45)	0.14	-	-	-
2FGLJ1054.5+2212	J105430.63+221055.0	BZBJ1054+2210	0.8 (0.04)	2.05(0.12)	2.47(0.28)	?	-	-	-
2FGLJ1057.0-8004	J105843.34-800354.1	BZBJ1058-8003	1.04(0.03)	2.8 (0.03)	2.23(0.04)	0.581	-	-	-
2FGLJ1057.1+7001	J105653.61+701145.9	BZQJ1056+7011	1.24(0.05)	3.4 (0.06)	2.54(0.13)	2.492	-	-	-
2FGLJ1058.6+5628	J105837.73+562811.3	BZBJ1058+5628	0.79(0.03)	2.27(0.03)	1.98(0.05)	0.143	BZB	B	0
2FGLJ1059.3-1132	J105912.43-113422.6	BZBJ1059-1134	0.98(0.03)	2.61(0.03)	2.15(0.05)	?	UND	C	0
2FGLJ1059.4+8113	J105811.54+811432.7	BZQJ1058+8114	1.15(0.03)	3.11(0.03)	2.46(0.06)	0.706	BZQ	B	0
2FGLJ1103.4-2330	J110337.62-232931.0	BZBJ1103-2329	0.54(0.03)	1.8 (0.08)	1.83(0.33)	0.186	-	-	-
2FGLJ1104.3+0729	J110424.07+073053.3	BZBJ1104+0730	0.91(0.04)	2.63(0.05)	1.93(0.15)	?	BZB	C	1
2FGLJ1104.4+3812	J110427.32+381231.9	BZBJ1104+3812	0.6 (0.03)	1.98(0.02)	1.85(0.03)	0.03	BZB	A	0
2FGLJ1106.1+2814	J110607.26+281247.1	BZQJ1106+2812	1.16(0.03)	3.01(0.04)	2.41(0.06)	0.844	BZQ	B	0
2FGLJ1107.2-4448	J110708.70-444907.6	BZQJ1107-4449	1.19(0.03)	3.05(0.03)	2.42(0.04)	1.598	BZQ	A	0
2FGLJ1107.5+0223	J110735.91+022224.5	BZBJ1107+0222	0.88(0.04)	2.24(0.11)	2.19(0.41)	?	-	-	-
2FGLJ1110.2+7134	J111037.60+713356.6	BZBJ1110+7133	0.83(0.04)	2.23(0.06)	2.13(0.23)	?	BZB	C	0
2FGLJ1112.4+3450	J111238.78+344639.1	BZQJ1112+3446	1.16(0.04)	3.11(0.05)	2.38(0.1)	1.956	BZQ	C	0
2FGLJ1117.2+2013	J111706.26+201407.5	BZBJ1117+2014	0.6 (0.03)	2.04(0.05)	1.92(0.18)	0.138	BZB	C	0
2FGLJ1118.1-4629	J111826.96-463415.0	BZQJ1118-4634	1.17(0.03)	2.87(0.03)	2.63(0.04)	0.713	BZQ	A	0
2FGLJ1121.0+4211	J112048.06+421212.6	BZBJ1120+4212	0.7 (0.03)	1.97(0.07)	1.59(0.34)	0.124??	BZB	C	0
2FGLJ1124.2+2338	J112402.71+233645.9	BZBJ1124+2336	1.19(0.04)	3.05(0.06)	2.42(0.15)	?	BZQ	C	0
2FGLJ1125.6-3559	J112531.49-355703.3	BZBJ1125-3557	0.87(0.03)	2.47(0.04)	2.09(0.1)	0.284	BZB	B	1
2FGLJ1126.0-0743	J112551.98-074220.9	BZBJ1125-0742	0.59(0.04)	1.77(0.13)	2.26(0.45)	0.279	-	-	-
2FGLJ1126.6-1856	J112704.40-185717.3	BZQJ1127-1857	1.1 (0.03)	2.94(0.03)	2.42(0.04)	1.048	-	-	-
2FGLJ1127.6+3622	J112758.88+362028.4	BZQJ1127+3620	1.06(0.06)	2.77(0.14)	2.41(0.4)	0.884	-	-	-
2FGLJ1130.3-1448	J113007.05-144927.4	BZQJ1130-1449	1.32(0.03)	2.85(0.03)	2.58(0.05)	1.184	BZQ	B	0
2FGLJ1130.9+5809	J113118.62+580858.9	BZBJ1131+5808	0.81(0.03)	2.29(0.04)	2.03(0.11)	0.36	BZB	B	0
2FGLJ1132.9+0033	J113245.62+003427.7	BZBJ1132+0034	0.93(0.03)	2.54(0.05)	1.95(0.16)	1.223??	BZB	C	1

*Continued on next page*

TABLE 8 – *Continued from previous page*

2FGL name	<i>WISE</i> name	ROMA-BZCAT name	[3.4]-[4.6] mag	[4.6]-[12] mag	[12]-[22] mag	z	type	class	$N_{BR}$
2FGLJ1136.3+6736	J113630.10+673704.4	BZBJ1136+6737	0.44(0.03)	1.87(0.06)	1.65(0.33)	0.136	-	-	-
2FGLJ1136.7+7009	J113626.42+700927.1	BZBJ1136+7009	0.41(0.03)	1.95(0.03)	2.0 (0.06)	0.045	-	-	-
2FGLJ1137.0+2553	J113650.11+255052.4	BZBJ1136+2550	0.37(0.04)	2.45(0.07)	1.96(0.32)	0.156	-	-	-
2FGLJ1143.1+6119	J114312.12+612210.8	BZBJ1143+6122	0.81(0.03)	2.26(0.04)	2.02(0.09)	?	BZB	B	0
2FGLJ1146.8-3812	J114701.37-381211.0	BZBJ1147-3812	1.13(0.03)	3.09(0.03)	2.47(0.05)	1.048?	BZQ	B	0
2FGLJ1146.9+4000	J114658.31+395834.4	BZQJ1146+3958	1.14(0.03)	3.0 (0.03)	2.41(0.05)	1.089	BZQ	B	0
2FGLJ1147.7-0724	J114751.56-072441.2	BZQJ1147-0724	1.08(0.04)	2.92(0.07)	2.94(0.13)	1.342	-	-	-
2FGLJ1150.1+2419	J115019.22+241753.9	BZBJ1150+2417	1.01(0.03)	2.67(0.03)	2.2 (0.03)	?	UND	A	0
2FGLJ1150.5+4154	J115034.76+415440.0	BZBJ1150+4154	0.8 (0.03)	2.29(0.04)	1.63(0.18)	?	-	-	-
2FGLJ1151.5+5857	J115124.66+585917.6	BZBJ1151+5859	0.79(0.03)	2.15(0.04)	1.84(0.14)	?	BZB	B	0
2FGLJ1152.4-0840	J115217.21-084103.1	BZQJ1152-0841	1.2 (0.04)	3.13(0.05)	2.57(0.1)	2.37	BZQ	C	0
2FGLJ1154.0-0010	J115404.56-001009.6	BZBJ1154-0010	0.53(0.05)	1.97(0.21)	3.15(0.36)	0.254	-	-	-
2FGLJ1154.4+6019	J115404.56+602220.9	BZQJ1154+6022	1.23(0.05)	2.79(0.08)	2.96(0.14)	1.12	-	-	-
2FGLJ1159.3-2142	J115921.42-214245.0	BZQJ1159-2142	1.1 (0.04)	2.81(0.04)	2.4 (0.1)	0.617	-	-	-
2FGLJ1159.5+2914	J115931.84+291443.9	BZQJ1159+2914	1.09(0.03)	3.0 (0.03)	2.42(0.04)	0.725	BZQ	A	0
2FGLJ1203.2+6030	J120303.53+603119.3	BZBJ1203+6031	0.67(0.03)	2.26(0.03)	1.94(0.05)	0.065	BZB	B	0
2FGLJ1204.3-0711	J120416.67-071008.8	BZBJ1204-0710	0.59(0.03)	1.95(0.06)	1.78(0.3)	0.184	BZB	C	0
2FGLJ1206.0-2638	J120533.21-263404.4	BZQJ1205-2634	1.13(0.03)	2.37(0.04)	2.07(0.13)	0.789	-	-	-
2FGLJ1208.8+5441	J120854.26+544158.2	BZQJ1208+5441	1.14(0.04)	2.83(0.05)	2.55(0.1)	1.345	BZQ	C	1
2FGLJ1209.6+4121	J120922.80+411941.4	BZBJ1209+4119	0.94(0.03)	2.56(0.04)	2.1 (0.09)	?	BZB	B	0
2FGLJ1209.7+1807	J120951.77+181006.7	BZQJ1209+1810	0.96(0.05)	2.64(0.11)	2.67(0.28)	0.845	-	-	-
2FGLJ1214.6+1309	J121332.18+130720.9	BZQJ1213+1307	0.99(0.05)	2.83(0.09)	2.52(0.22)	1.139	-	-	-
2FGLJ1214.8+1653	J121503.99+165437.9	BZQJ1215+1654	1.01(0.05)	3.14(0.08)	2.53(0.18)	1.132	BZQ	C	0
2FGLJ1214.9+5004	J121500.80+500215.5	BZBJ1215+5002	0.91(0.04)	2.46(0.05)	2.13(0.17)	?	BZB	C	2
2FGLJ1217.8+3006	J121752.08+300700.7	BZBJ1217+3007	0.83(0.03)	2.32(0.03)	2.02(0.04)	0.13?	BZB	A	0
2FGLJ1218.5-0122	J121834.94-011954.2	BZBJ1218-0119	0.91(0.03)	2.44(0.04)	2.18(0.08)	?	BZB	B	0
2FGLJ1219.2+7107	J122003.64+710531.2	BZQJ1220+7105	1.14(0.06)	3.03(0.09)	2.54(0.25)	0.451	BZQ	C	1
2FGLJ1219.7+0201	J122011.89+020342.3	BZQJ1220+0203	0.98(0.03)	2.27(0.03)	2.34(0.06)	0.241	BZB	B	1
2FGLJ1219.8-0310	J121945.71-031423.8	BZBJ1219-0314	0.71(0.04)	2.23(0.1)	2.65(0.22)	0.299	-	-	-
2FGLJ1221.3+3010	J122121.95+301037.2	BZBJ1221+3010	0.67(0.03)	2.05(0.04)	1.9 (0.13)	0.182	BZB	B	0
2FGLJ1221.4+2814	J122131.69+281358.5	BZBJ1221+2813	0.85(0.03)	2.32(0.03)	2.0 (0.03)	0.102	BZB	A	0
2FGLJ1222.4+0413	J122222.55+041315.8	BZQJ1222+0413	1.11(0.03)	2.7 (0.04)	2.35(0.08)	0.966	UND	B	0
2FGLJ1223.9+8043	J122340.50+804004.4	BZBJ1223+8040	1.09(0.03)	2.97(0.03)	2.37(0.07)	?	BZQ	B	0
2FGLJ1224.4+2436	J122424.20+243623.6	BZBJ1224+2436	0.75(0.04)	2.08(0.08)	2.08(0.31)	0.218	BZB	C	0
2FGLJ1224.9+2122	J122454.46+212246.4	BZQJ1224+2122	1.06(0.03)	2.57(0.03)	2.13(0.03)	0.435	UND	A	0
2FGLJ1225.0+4335	J122451.51+433519.4	BZBJ1224+4335	0.98(0.05)	2.72(0.08)	2.63(0.1)	?	-	-	-
2FGLJ1226.7-1331	J122654.42-132838.8	BZBJ1226-1328	1.05(0.04)	2.81(0.04)	2.34(0.1)	0.456	UND	B	0
2FGLJ1228.6+4857	J122851.77+485801.5	BZQJ1228+4858	1.21(0.06)	3.14(0.1)	2.97(0.17)	1.722	-	-	-
2FGLJ1229.1+0202	J122906.70+020308.6	BZQJ1229+0203	0.96(0.03)	2.26(0.02)	2.2 (0.02)	0.158	BZB	A	0
2FGLJ1230.2+2517	J123014.09+251807.1	BZBJ1230+2518	0.97(0.03)	2.58(0.03)	2.08(0.04)	0.135??	BZB	A	0
2FGLJ1231.7+2848	J123143.57+284749.8	BZBJ1231+2847	0.86(0.03)	2.32(0.03)	1.96(0.05)	0.236?	BZB	B	0
2FGLJ1233.7-0145	J123341.34-014423.6	BZBJ1233-0144	1.01(0.05)	2.62(0.1)	1.8 (0.47)	?	-	-	-
2FGLJ1239.5+0443	J123932.76+044305.3	BZQJ1239+0443	1.14(0.04)	2.91(0.06)	2.04(0.17)	1.762	-	-	-
2FGLJ1241.6-1457	J124149.40-145558.4	BZBJ1241-1455	0.68(0.03)	2.03(0.06)	1.88(0.24)	?	BZB	C	0
2FGLJ1243.1+3627	J124312.74+362744.0	BZBJ1243+3627	0.78(0.03)	2.2 (0.03)	1.87(0.09)	?	BZB	B	0
2FGLJ1245.1+5708	J124510.03+570954.3	BZBJ1245+5709	0.91(0.03)	2.55(0.04)	2.27(0.08)	?	BZB	C	2
2FGLJ1246.7-2546	J124646.81-254749.1	BZQJ1246-2547	1.1 (0.03)	2.91(0.03)	2.41(0.04)	0.635	BZQ	A	0
2FGLJ1248.2+5820	J124818.79+582028.8	BZBJ1248+5820	0.86(0.03)	2.29(0.03)	1.9(0.04)	?	BZB	A	0
2FGLJ1251.2+1045	J125117.89+103907.1	BZBJ1251+1039	0.73(0.04)	2.07(0.07)	1.81(0.31)	0.245	BZB	C	0
2FGLJ1253.1+5302	J125311.91+530111.8	BZBJ1253+5301	0.93(0.03)	2.55(0.03)	2.1 (0.05)	?	BZB	B	0
2FGLJ1254.1+6237	J125359.34+624257.6	BZBJ1253+6242	0.85(0.04)	2.33(0.07)	2.19(0.23)	?	BZB	C	0
2FGLJ1254.4+2209	J125433.28+221103.9	BZBJ1254+2211	0.77(0.03)	2.16(0.05)	2.15(0.17)	?	BZB	C	0
2FGLJ1256.1-0547	J125611.17-054721.5	BZQJ1256-0547	1.31(0.03)	3.14(0.03)	2.7(0.03)	0.536	BZQ	C	0
2FGLJ1257.0+3650	J125716.58+364715.0	BZBJ1257+3647	0.8 (0.03)	2.26(0.05)	2.06(0.16)	0.531	BZB	C	1
2FGLJ1258.2+3231	J125757.23+322929.3	BZQJ1257+3229	1.01(0.03)	2.65(0.03)	2.26(0.05)	0.806	UND	B	0
2FGLJ1258.4-1801	J125838.32-180003.1	BZQJ1258-1800	0.98(0.05)	2.84(0.08)	2.68(0.18)	1.956	-	-	-
2FGLJ1258.8-2223	J125854.48-221931.1	BZQJ1258-2219	1.19(0.03)	2.95(0.03)	2.41(0.06)	1.303	BZQ	B	0
2FGLJ1303.1+2435	J130303.21+243355.7	BZBJ1303+2433	1.06(0.04)	2.82(0.05)	2.27(0.11)	0.993	UND	C	0
2FGLJ1303.5-4622	J130340.28-462102.3	BZQJ1303-4621	1.08(0.03)	2.86(0.04)	2.23(0.08)	1.664	UND	B	0
2FGLJ1308.5+3547	J130823.73+354637.1	BZQJ1308+3546	1.07(0.05)	3.08(0.06)	2.63(0.14)	1.055	BZQ	C	0
2FGLJ1309.3+1154	J130933.93+115424.6	BZBJ1309+1154	1.08(0.03)	2.77(0.04)	2.29(0.08)	?	UND	B	0
2FGLJ1309.4+4304	J130925.52+430505.6	BZBJ1309+4305	0.89(0.03)	2.36(0.04)	1.88(0.1)	?	BZB	B	0
2FGLJ1310.9+0036	J131106.47+003510.0	BZBJ1311+0035	0.79(0.04)	2.11(0.1)	2.22(0.35)	?	BZB	C	0
2FGLJ1312.4-2157	J131231.56-215623.3	BZBJ1312-2156	0.92(0.03)	2.35(0.03)	1.92(0.07)	1.491?	BZB	B	0
2FGLJ1313.0-0425	J131250.90-042449.9	BZQJ1312-0424	0.98(0.07)	3.42(0.11)	2.39(0.32)	0.825	-	-	-
2FGLJ1314.6+2348	J131443.81+234826.7	BZBJ1314+2348	0.87(0.03)	2.31(0.03)	1.95(0.05)	?	BZB	B	0
2FGLJ1315.9-3339	J131607.99-333859.1	BZQJ1316-3338	1.12(0.03)	3.09(0.03)	2.3 (0.06)	1.21	BZQ	B	1
2FGLJ1317.9+3426	J131736.49+342516.0	BZQJ1317+3425	1.11(0.03)	2.89(0.04)	2.26(0.08)	1.05	UND	C	1
2FGLJ1321.1+2215	J132111.21+221612.1	BZQJ1321+2216	1.15(0.04)	3.08(0.04)	2.47(0.07)	0.943	BZQ	B	0
2FGLJ1326.8+2210	J132700.87+221050.2	BZQJ1327+2210	1.17(0.04)	3.13(0.05)	2.45(0.1)	1.4?	BZQ	C	0
2FGLJ1330.9+7001	J133025.81+700138.7	BZBJ1330+7001	0.83(0.04)	2.14(0.07)	2.29(0.21)	?	BZB	C	0
2FGLJ1332.0-0508	J133204.47-050943.1	BZQJ1332-0509	1.27(0.03)	3.33(0.03)	2.57(0.05)	2.15	BZQ	C	0
2FGLJ1332.5-1255	J133239.26-125615.3	BZQJ1332-1256	1.26(0.07)	2.97(0.15)	2.45(0.43)	1.498	-	-	-
2FGLJ1332.7+2726	J133307.50+272518.3	BZQJ1333+2725	0.91(0.04)	2.95(0.06)	2.56(0.14)	2.126	-	-	-
2FGLJ1332.7+4725	J133245.22+472222.5	BZQJ1332+4722	0.94(0.04)	3.02(0.07)	2.59(0.17)	0.668	-	-	-

*Continued on next page*

TABLE 8 – *Continued from previous page*

2FGL name	WISE name	ROMA-BZCAT name	[3.4]-[4.6] mag	[4.6]-[12] mag	[12]-[22] mag	z	type	class	N <sub>BR</sub>
2FGLJ1337.7-1257	J133739.79-125724.5	BZQJ1337-1257	1.16(0.03)	3.12(0.03)	2.55(0.03)	0.539	BZQ	A	0
2FGLJ1338.9+1152	J133859.06+115316.7	BZBJ1338+1153	0.92(0.04)	2.28(0.06)	2.35(0.19)	?	BZB	C	0
2FGLJ1340.5+4407	J134029.82+441003.9	BZBJ1340+4410	0.35(0.04)	1.06(0.32)	3.67(0.44)	0.546	-	-	-
2FGLJ1341.3-2048	J134204.74-205129.3	BZQJ1342-2051	1.45(0.05)	3.1 (0.07)	2.44(0.14)	1.582	-	-	-
2FGLJ1344.2-1723	J134414.40-172340.2	BZQJ1344-1723	1.12(0.03)	2.96(0.04)	2.31(0.07)	2.49	BZQ	C	0
2FGLJ1345.4+4453	J134533.17+445259.6	BZQJ1345+4452	1.2 (0.09)	3.28(0.16)	3.09(0.28)	2.534	-	-	-
2FGLJ1345.9+0706	J134549.32+070631.2	BZQJ1345+0706	1.09(0.03)	2.89(0.04)	2.36(0.08)	1.093	UND	C	3
2FGLJ1347.7-3752	J134740.43-375036.5	BZQJ1347-3750	1.03(0.03)	2.77(0.04)	2.14(0.11)	1.3	UND	B	0
2FGLJ1351.1+0032	J135104.45+003119.6	BZQJ1351+0031	1.07(0.04)	2.68(0.08)	2.39(0.23)	2.084	UND	C	3
2FGLJ1351.4+1115	J135120.85+111453.1	BZBJ1351+1114	0.66(0.04)	2.06(0.07)	1.88(0.3)	?	BZB	C	1
2FGLJ1352.6-4413	J135256.54-441240.2	BZBJ1352-4412	1.04(0.03)	2.8 (0.03)	2.25(0.04)	?	UND	B	0
2FGLJ1353.3+1435	J135322.84+143539.3	BZBJ1353+1435	0.99(0.03)	2.89(0.04)	2.41(0.09)	?	UND	B	0
2FGLJ1354.5+3703	J135426.70+370654.6	BZBJ1354+3706	0.76(0.03)	2.14(0.05)	2.08(0.15)	?	BZB	B	0
2FGLJ1354.7-1047	J135446.52-104102.5	BZQJ1354-1041	0.98(0.03)	3.02(0.04)	2.51(0.07)	0.33	BZQ	C	2
2FGLJ1358.0+0137	J135738.70+012813.7	BZBJ1357+0128	0.82(0.04)	2.38(0.06)	2.28(0.18)	?	BZB	C	8
2FGLJ1358.1+7644	J135755.39+764321.1	BZQJ1357+7643	1.16(0.04)	2.89(0.07)	2.88(0.13)	1.585	-	-	-
2FGLJ1359.4+5541	J135905.74+554429.4	BZQJ1359+5544	1.02(0.03)	2.8 (0.04)	2.38(0.08)	1.014	UND	B	1
2FGLJ1359.9-3746	J135949.72-374600.7	BZBJ1359-3746	0.85(0.03)	2.46(0.04)	2.03(0.09)	?	BZB	B	1
2FGLJ1408.8-0751	J140856.48-075226.5	BZQJ1408-0752	1.22(0.04)	2.96(0.04)	2.58(0.07)	1.494	BZQ	B	0
2FGLJ1410.3+2811	J141029.56+282055.7	BZBJ1410+2820	0.71(0.04)	2.01(0.09)	2.16(0.38)	?	-	-	-
2FGLJ1418.1+2539	J141756.67+254325.9	BZBJ1417+2543	0.52(0.03)	2.01(0.05)	1.51(0.28)	0.237	BZB	C	4
2FGLJ1418.4-0234	J141826.33-023334.0	BZBJ1418-0233	0.85(0.03)	2.2 (0.03)	1.86(0.06)	?	BZB	B	0
2FGLJ1419.4+3820	J141946.61+382148.5	BZQJ1419+3821	1.21(0.04)	3.21(0.04)	2.51(0.08)	1.831	BZQ	B	1
2FGLJ1420.2+5422	J141946.60+542314.8	BZBJ1419+5423	0.94(0.03)	2.54(0.02)	2.13(0.03)	0.153	BZB	A	0
2FGLJ1425.1+3615	J142455.51+361536.0	BZBJ1424+3615	0.9 (0.04)	2.36(0.07)	1.75(0.36)	?	-	-	-
2FGLJ1426.1+3406	J142607.73+340426.4	BZBJ1426+3404	0.89(0.03)	2.42(0.04)	2.07(0.12)	?	BZB	B	0
2FGLJ1427.0+2347	J142700.40+234800.1	BZBJ1427+2348	0.82(0.03)	2.24(0.02)	1.9(0.03)	?	BZB	A	0
2FGLJ1427.4-3306	J142741.36-330531.5	BZBJ1427-3305	1.12(0.03)	2.95(0.03)	2.46(0.04)	?	BZQ	A	0
2FGLJ1428.0-4206	J142756.30-420619.3	BZQJ1427-4206	1.08(0.03)	2.93(0.02)	2.37(0.03)	1.522	BZQ	C	0
2FGLJ1428.6+4240	J142832.62+424021.0	BZBJ1428+4240	0.5 (0.03)	1.79(0.05)	1.55(0.28)	0.129	-	-	-
2FGLJ1433.8+4205	J143405.70+420315.9	BZQJ1434+4203	1.01(0.05)	2.77(0.08)	2.53(0.22)	1.24	UND	C	2
2FGLJ1436.9+2319	J143640.99+232103.4	BZQJ1436+2321	1.23(0.04)	3.21(0.05)	2.74(0.08)	1.544	BZQ	C	0
2FGLJ1439.2+3932	J143917.48+393242.8	BZBJ1439+3932	0.71(0.03)	2.1 (0.04)	1.84(0.13)	0.344	BZB	B	1
2FGLJ1440.3+4948	J143946.98+495805.3	BZBJ1439+4958	1.13(0.03)	3.06(0.03)	2.5 (0.06)	?	BZQ	B	0
2FGLJ1440.9+0611	J144052.94+061016.2	BZBJ1440+0610	0.8 (0.03)	2.27(0.05)	1.94(0.17)	?	BZB	C	0
2FGLJ1442.0+4352	J144207.15+434836.7	BZBJ1442+4348	0.91(0.03)	2.41(0.05)	1.93(0.17)	?	BZB	C	0
2FGLJ1442.7+1159	J144248.24+120040.3	BZBJ1442+1200	0.48(0.03)	1.69(0.06)	1.67(0.33)	0.163	-	-	-
2FGLJ1443.9-3908	J144357.20-390839.9	BZBJ1443-3908	0.71(0.03)	2.14(0.03)	1.9 (0.08)	0.065?	BZB	B	0
2FGLJ1444.1+2500	J144356.90+250144.4	BZQJ1443+2501	0.99(0.05)	2.92(0.1)	2.73(0.23)	0.939	-	-	-
2FGLJ1448.0+3608	J144800.59+360831.2	BZBJ1448+3608	0.77(0.03)	2.13(0.04)	2.11(0.12)	?	BZB	B	0
2FGLJ1454.4+5123	J145427.13+512433.7	BZBJ1454+5124	0.91(0.03)	2.39(0.03)	2.03(0.06)	?	BZB	B	0
2FGLJ1457.4-3540	J145726.71-353909.8	BZQJ1457-3539	1.04(0.04)	2.83(0.04)	2.27(0.07)	1.424	UND	B	0
2FGLJ1501.0+2238	J150101.83+223806.3	BZBJ1501+2238	0.83(0.03)	2.27(0.03)	1.91(0.04)	0.235	BZB	B	0
2FGLJ1503.7-1541	J150340.67-154114.0	BZBJ1503-1541	0.64(0.04)	1.99(0.1)	2.19(0.39)	?	-	-	-
2FGLJ1504.3+1029	J150424.98+102939.2	BZQJ1504+1029	1.12(0.03)	2.89(0.03)	2.33(0.06)	1.839	UND	C	0
2FGLJ1504.9-3433	J150502.37-343256.9	BZBJ1505-3432	1.29(0.05)	3.09(0.07)	2.64(0.17)	?	BZQ	C	1
2FGLJ1506.0+3729	J150609.53+373051.1	BZQJ1506+3730	1.34(0.03)	2.89(0.04)	2.06(0.09)	0.674	-	-	-
2FGLJ1506.6+0806	J150644.47+081400.8	BZBJ1506+0814	0.72(0.03)	2.2 (0.05)	2.03(0.15)	0.376?	BZB	B	0
2FGLJ1508.5+2709	J150842.69+270909.0	BZBJ1508+2709	0.43(0.04)	1.85(0.1)	2.38(0.3)	0.27	-	-	-
2FGLJ1508.9-4342	J150935.73-434032.1	BZQJ1509-4340	1.04(0.05)	2.66(0.07)	2.72(0.18)	0.776	-	-	-
2FGLJ1509.7+5556	J150947.96+555617.3	BZBJ1509+5556	0.8 (0.03)	2.24(0.05)	2.02(0.16)	?	BZB	C	2
2FGLJ1510.9-0545	J151053.59-054307.3	BZQJ1510-0543	1.13(0.03)	2.91(0.04)	2.56(0.06)	1.191	BZQ	B	0
2FGLJ1512.8-0906	J151250.53-090559.7	BZQJ1512-0905	1.05(0.03)	2.7 (0.03)	2.38(0.03)	0.36	UND	A	0
2FGLJ1514.6+4449	J151436.65+445004.3	BZQJ1514+4450	0.99(0.03)	2.56(0.03)	2.16(0.07)	0.57	UND	C	2
2FGLJ1516.9+1925	J151656.80+193213.0	BZBJ1516+1932	1.05(0.03)	2.87(0.03)	2.36(0.04)	?	UND	B	0
2FGLJ1517.7-2421	J151741.82-242219.4	BZBJ1517-2422	0.86(0.03)	2.59(0.03)	2.19(0.03)	0.048	BZB	A	0
2FGLJ1518.0+6526	J151747.59+652523.3	BZBJ1517+6525	0.72(0.03)	1.94(0.06)	1.95(0.21)	0.702	BZB	C	0
2FGLJ1520.8-0349	J152048.91-034851.5	BZBJ1520-0348	0.81(0.03)	2.2 (0.05)	1.9 (0.16)	?	BZB	C	0
2FGLJ1522.0+4348	J152149.61+433639.2	BZQJ1521+4336	1.13(0.05)	3.2 (0.07)	2.32(0.21)	2.171	BZQ	C	5
2FGLJ1522.1+3144	J152210.00+314414.4	BZQJ1522+3144	1.2 (0.05)	2.86(0.08)	2.84(0.18)	1.487	-	-	-
2FGLJ1522.7-2731	J152237.68-273010.6	BZBJ1522-2730	0.97(0.04)	2.82(0.07)	2.2 (0.18)	?	UND	C	0
2FGLJ1531.0+5725	J153058.21+573625.3	BZBJ1530+5736	0.85(0.04)	2.05(0.12)	2.61(0.32)	?	-	-	-
2FGLJ1535.4+3720	J153447.21+371554.8	BZBJ1534+3715	0.54(0.04)	1.97(0.08)	2.03(0.36)	0.143	BZB	C	2
2FGLJ1538.1+8159	J154015.90+815505.6	BZBJ1540+8155	0.68(0.03)	1.99(0.04)	1.85(0.16)	?	-	-	-
2FGLJ1539.5+2747	J153939.14+274438.2	BZQJ1539+2744	1.21(0.04)	3.05(0.06)	2.31(0.16)	2.19	BZQ	C	0
2FGLJ1540.4+1438	J154049.49+144746.0	BZBJ1540+1447	1.03(0.03)	2.85(0.03)	2.34(0.05)	0.605	UND	B	0
2FGLJ1542.9+6129	J154256.94+612955.3	BZBJ1542+6129	0.88(0.03)	2.36(0.03)	1.97(0.03)	?	BZB	A	0
2FGLJ1546.1+0820	J154604.26+081913.5	BZBJ1546+0819	0.8 (0.04)	2.2 (0.08)	1.68(0.4)	?	BZB	C	2
2FGLJ1548.8-2251	J154849.76-225102.5	BZBJ1548-2251	0.65(0.03)	2.04(0.05)	1.69(0.28)	?	BZB	C	0
2FGLJ1549.5+0237	J154929.44+023701.2	BZQJ1549+0237	1.04(0.03)	2.6 (0.03)	2.31(0.05)	0.414	UND	B	0
2FGLJ1550.7+0526	J155035.27+052710.6	BZQJ1550+0527	1.19(0.04)	3.11(0.04)	2.49(0.07)	1.422	BZQ	B	0
2FGLJ1551.9+0855	J155203.26+085047.4	BZBJ1552+0850	0.96(0.03)	2.69(0.03)	2.19(0.06)	?	UND	B	0
2FGLJ1553.5+1255	J155332.70+125651.7	BZQJ1553+1256	1.27(0.05)	3.11(0.08)	2.34(0.21)	1.308	BZQ	C	0
2FGLJ1553.5-3116	J155333.56-311830.9	BZBJ1553-3118	0.69(0.03)	2.17(0.04)	2.07(0.11)	?	BZB	B	0
2FGLJ1555.7+1111	J155543.05+111124.4	BZBJ1555+1111	0.8 (0.03)	2.14(0.03)	1.85(0.05)	?	BZB	B	0

*Continued on next page*

TABLE 8 – *Continued from previous page*

2FGL name	WISE name	ROMA-BZCAT name	[3.4]-[4.6] mag	[4.6]-[12] mag	[12]-[22] mag	z	type	class	$N_{BR}$
2FGLJ1559.0+5627	J155848.30+562514.1	BZBJ1558+5625	0.98(0.03)	2.59(0.03)	2.16(0.04)	0.3	UND	C	4
2FGLJ1604.6+5710	J160437.36+571436.6	BZQJ1604+5714	1.11(0.03)	2.94(0.03)	2.51(0.04)	0.72	BZQ	A	0
2FGLJ1607.0+1552	J160706.43+155134.8	BZBJ1607+1551	1.01(0.03)	2.84(0.04)	2.52(0.08)	?	UND	C	0
2FGLJ1608.5+1029	J160846.20+102907.8	BZQJ1608+1029	1.09(0.03)	2.8(0.03)	2.41(0.05)	1.226	UND	C	0
2FGLJ1610.8-6650	J161046.45-664901.1	BZBJ1610-6649	0.74(0.03)	2.06(0.04)	1.64(0.16)	?	BZB	C	0
2FGLJ1613.4+3409	J161341.07+341248.0	BZQJ1613+3412	1.14(0.04)	2.9(0.05)	2.57(0.12)	1.397	BZQ	C	0
2FGLJ1618.2-7718	J161749.28-771718.3	BZQJ1617-7717	1.05(0.04)	3.01(0.04)	2.45(0.07)	1.71	BZQ	B	0
2FGLJ1630.4+5218	J163043.14+522138.7	BZBJ1630+5221	0.81(0.03)	2.17(0.04)	1.96(0.12)	?	BZB	B	0
2FGLJ1635.2+3810	J163515.50+380804.5	BZQJ1635+3808	1.21(0.03)	3.33(0.03)	2.6(0.04)	1.814	-	-	-
2FGLJ1637.7+4714	J163745.14+471733.8	BZQJ1637+4717	1.18(0.03)	3.07(0.03)	2.44(0.04)	0.735	BZQ	A	0
2FGLJ1640.7+3945	J164029.64+394646.1	BZQJ1640+3946	1.12(0.05)	3.14(0.08)	2.49(0.19)	1.66	-	-	-
2FGLJ1641.6-0614	J164202.18-062123.5	BZBJ1642-0621	1.1(0.04)	3.05(0.04)	2.46(0.07)	?	-	-	-
2FGLJ1649.6+5238	J164925.00+523515.0	BZBJ1649+5235	0.82(0.03)	2.35(0.03)	1.95(0.07)	?	BZB	B	0
2FGLJ1650.8+0830	J165037.56+082452.4	BZQJ1650+0824	1.2(0.04)	3.13(0.05)	2.29(0.14)	1.965	BZQ	C	3
2FGLJ1653.9+3945	J165352.22+394536.5	BZBJ1653+3945	0.46(0.03)	2.01(0.03)	2.0(0.03)	0.033	BZB	C	0
2FGLJ1700.2+6831	J170009.29+683007.0	BZQJ1700+6830	1.03(0.03)	2.64(0.03)	2.18(0.02)	0.301	UND	A	0
2FGLJ1703.2-6217	J170336.55-621239.9	BZQJ1703-6212	0.97(0.03)	2.81(0.03)	2.28(0.04)	1.75	-	-	-
2FGLJ1709.7+4319	J170941.09+431844.6	BZQJ1709+4318	1.14(0.04)	3.0(0.04)	2.44(0.07)	1.027	BZQ	B	0
2FGLJ1714.8+6836	J171613.93+683638.8	BZQJ1716+6836	1.01(0.03)	2.75(0.03)	2.3(0.04)	0.777	-	-	-
2FGLJ1719.3+1744	J171913.05+174506.5	BZBJ1719+1745	1.08(0.03)	2.87(0.03)	2.26(0.05)	0.137?	UND	B	0
2FGLJ1722.7+1013	J172244.58+101335.9	BZQJ1722+1013	1.06(0.03)	2.95(0.03)	2.41(0.04)	0.732	BZQ	C	0
2FGLJ1724.0+4003	J172405.42+400436.5	BZQJ1724+4004	1.07(0.04)	3.04(0.05)	2.38(0.11)	1.049	BZQ	C	0
2FGLJ1725.0+1151	J172504.34+115215.5	BZBJ1725+1152	0.78(0.03)	2.13(0.03)	1.83(0.08)	?	BZB	B	0
2FGLJ1725.2+5853	J172535.02+585140.0	BZBJ1725+5851	0.9(0.03)	2.46(0.03)	1.93(0.07)	?	BZB	B	1
2FGLJ1727.1+4531	J172727.66+453039.7	BZQJ1727+4530	1.15(0.03)	3.1(0.03)	2.6(0.06)	0.717	BZQ	B	0
2FGLJ1727.9+1220	J172807.05+121539.6	BZQJ1728+1215	1.14(0.04)	2.97(0.04)	2.53(0.08)	0.583	BZQ	B	1
2FGLJ1728.2+0429	J172824.95+042704.9	BZQJ1728+0427	0.97(0.03)	2.82(0.03)	2.64(0.04)	0.293	-	-	-
2FGLJ1728.2+5015	J172818.63+501310.5	BZBJ1728+5013	0.62(0.03)	2.18(0.03)	2.05(0.07)	0.055	BZB	B	0
2FGLJ1730.7+0023	J173035.00+002438.8	BZQJ1730+0024	1.07(0.03)	2.89(0.03)	2.34(0.07)	1.335	UND	C	0
2FGLJ1731.3+3718	J173047.05+371455.2	BZBJ1730+3714	0.7(0.03)	2.28(0.04)	2.18(0.13)	?	BZB	B	1
2FGLJ1733.1-1307	J173302.71-130449.5	BZQJ1733-1304	1.02(0.03)	2.85(0.03)	2.53(0.05)	0.902	BZQ	B	0
2FGLJ1734.3+3858	J173420.58+385751.4	BZQJ1734+3857	1.16(0.03)	3.17(0.03)	2.37(0.06)	0.976	BZQ	B	0
2FGLJ1739.5+4955	J173927.39+495503.4	BZQJ1739+4955	1.08(0.03)	2.83(0.03)	2.33(0.04)	1.545	UND	B	0
2FGLJ1740.2+5212	J174036.97+521143.4	BZQJ1740+5211	1.16(0.03)	2.97(0.03)	2.33(0.03)	1.381	BZQ	A	0
2FGLJ1740.3+4738	J173957.13+473758.4	BZBJ1739+4737	1.07(0.03)	2.91(0.03)	2.36(0.06)	?	UND	C	1
2FGLJ1742.1+5948	J174232.00+594506.7	BZBJ1742+5945	0.94(0.03)	2.54(0.03)	2.04(0.05)	?	BZB	B	0
2FGLJ1744.1+1934	J174357.84+193509.3	BZBJ1743+1935	0.42(0.03)	1.87(0.04)	1.94(0.11)	0.084	BZB	C	0
2FGLJ1745.5-0751	J174527.10-075303.7	BZBJ1745-0753	0.88(0.04)	2.63(0.04)	2.34(0.09)	?	UND	B	0
2FGLJ1748.8+7006	J174832.85+700550.7	BZBJ1748+7005	1.02(0.03)	2.73(0.02)	2.24(0.03)	0.77?	UND	A	0
2FGLJ1749.1+4323	J174900.36+432151.4	BZBJ1749+4321	1.11(0.03)	3.02(0.03)	2.36(0.06)	?	BZQ	B	1
2FGLJ1754.3+3212	J175411.80+321223.1	BZBJ1754+3212	0.85(0.03)	2.27(0.03)	1.94(0.07)	?	BZB	B	0
2FGLJ1756.5+5523	J175615.90+552218.0	BZBJ1756+5522	0.6(0.04)	1.85(0.1)	2.1(0.47)	?	-	-	-
2FGLJ1800.5+7829	J180045.70+782804.1	BZBJ1800+7828	1.12(0.03)	2.94(0.02)	2.32(0.03)	0.68	BZQ	B	0
2FGLJ1801.7+4405	J180132.33+440421.8	BZQJ1801+4404	1.02(0.03)	3.0(0.03)	2.5(0.05)	0.663	BZQ	B	0
2FGLJ1806.7+6948	J180650.69+694928.1	BZBJ1806+6949	0.85(0.03)	2.47(0.02)	2.08(0.03)	0.046	BZB	A	0
2FGLJ1809.7+2909	J180945.39+291019.9	BZBJ1809+2910	0.95(0.03)	2.55(0.03)	2.07(0.06)	?	BZB	B	1
2FGLJ1810.8+1606	J181050.18+160820.8	BZBJ1810+1608	0.88(0.04)	2.33(0.07)	2.09(0.28)	?	BZB	C	0
2FGLJ1811.3+0339	J181118.02+034113.7	BZBJ1811+0341	0.67(0.03)	1.97(0.07)	1.61(0.33)	?	BZB	C	0
2FGLJ1813.5+3143	J181335.20+314417.7	BZBJ1813+3144	0.78(0.03)	2.17(0.04)	1.72(0.14)	0.117	BZB	C	0
2FGLJ1813.7+0617	J181333.41+061542.0	BZBJ1813+0615	0.99(0.04)	2.79(0.04)	2.33(0.08)	?	UND	B	0
2FGLJ1818.6+0903	J181840.06+090346.3	BZQJ1818+0903	1.02(0.04)	2.77(0.05)	2.32(0.09)	0.354	UND	C	1
2FGLJ1823.7+6856	J182332.64+685752.2	BZBJ1823+6857	0.85(0.03)	2.57(0.03)	2.34(0.07)	?	BZB	C	3
2FGLJ1824.0+5650	J182407.07+565101.5	BZBJ1824+5651	1.02(0.03)	2.94(0.03)	2.36(0.04)	0.664	UND	A	0
2FGLJ1829.2+5402	J182924.29+540259.7	BZBJ1829+5402	0.81(0.03)	2.12(0.04)	1.98(0.14)	?	BZB	B	0
2FGLJ1832.7-5700	J183230.98-565920.6	BZBJ1832-5659	0.96(0.04)	2.71(0.04)	2.37(0.09)	?	UND	B	1
2FGLJ1836.2+3137	J183621.23+313626.7	BZBJ1836+3136	0.8(0.03)	2.24(0.04)	1.98(0.14)	?	BZB	B	0
2FGLJ1838.7+4759	J183849.15+480234.4	BZBJ1838+4802	0.74(0.03)	2.03(0.04)	1.99(0.15)	?	BZB	B	0
2FGLJ1841.7+3221	J184147.04+321839.2	BZBJ1841+3218	0.72(0.04)	1.91(0.07)	1.66(0.42)	?	BZB	C	0
2FGLJ1848.5+3216	J184822.09+321902.7	BZQJ1848+3219	1.13(0.04)	3.0(0.04)	2.52(0.06)	0.798	BZQ	B	1
2FGLJ1849.4+6706	J184916.08+670541.5	BZQJ1849+6705	1.17(0.03)	3.09(0.03)	2.52(0.04)	0.657	BZQ	A	0
2FGLJ1849.7-4310	J184925.92-431413.2	BZBJ1849-4314	0.93(0.03)	2.51(0.03)	2.07(0.06)	?	BZB	B	0
2FGLJ1852.5+4856	J185228.55+485547.6	BZQJ1852+4855	1.05(0.03)	2.81(0.03)	2.3(0.06)	1.25	UND	B	0
2FGLJ1902.5-6746	J190301.23-674935.6	BZQJ1903-6749	1.07(0.03)	2.81(0.04)	2.44(0.09)	0.254	UND	C	2
2FGLJ1903.3+5539	J190311.60+554038.5	BZBJ1903+5540	0.9(0.03)	2.37(0.03)	2.03(0.04)	?	BZB	A	0
2FGLJ1917.6-1921	J191744.82-192131.5	BZBJ1917-1921	0.82(0.03)	2.24(0.03)	2.14(0.06)	0.137	BZB	B	0
2FGLJ1918.2-4110	J191816.05-411130.8	BZBJ1918-4111	0.97(0.04)	2.47(0.05)	2.23(0.1)	?	-	-	-
2FGLJ1921.9-1608	J192151.55-160713.2	BZBJ1921-1607	0.65(0.03)	3.52(0.03)	0.9(0.1)	?	-	-	-
2FGLJ1923.5-2105	J192332.17-210433.3	BZQJ1923-2104	1.09(0.03)	2.74(0.03)	2.36(0.04)	0.874	UND	B	0
2FGLJ1924.8-2912	J192451.05-291430.0	BZQJ1924-2914	1.13(0.03)	3.07(0.02)	2.48(0.02)	0.352	BZQ	A	0
2FGLJ1936.8-4721	J193656.10-471950.0	BZBJ1936-4719	0.63(0.04)	2.16(0.09)	2.34(0.26)	0.265	-	-	-
2FGLJ1946.1-3115	J194559.41-311139.3	BZBJ1945-3111	0.76(0.04)	2.38(0.05)	2.24(0.14)	?	BZB	C	1
2FGLJ1958.2-3848	J195759.81-384506.2	BZQJ1957-3845	1.14(0.03)	2.88(0.03)	2.44(0.05)	0.63	-	-	-
2FGLJ1959.1-4245	J195913.26-424607.4	BZQJ1959-4246	1.14(0.04)	2.94(0.04)	2.47(0.09)	2.174	BZQ	B	0
2FGLJ2000.0+6509	J195959.84+650854.7	BZBJ1959+6508	0.59(0.03)	2.12(0.03)	1.93(0.04)	0.047	BZB	A	0
2FGLJ2000.8-1751	J200057.09-174857.5	BZQJ2000-1748	1.12(0.03)	3.16(0.03)	2.58(0.05)	0.652	BZQ	B	0

*Continued on next page*

TABLE 8 – *Continued from previous page*

2FGL name	WISE name	ROMA-BZCAT name	[3.4]-[4.6] mag	[4.6]-[12] mag	[12]-[22] mag	z	type	class	$N_{BR}$
2FGLJ2004.5+7754	J200531.01+775243.2	BZBJ2005+7752	1.01(0.03)	2.7(0.03)	2.26(0.03)	0.342	UND	A	0
2FGLJ2009.5-4850	J200925.39-484953.5	BZBJ2009-4849	0.73(0.03)	2.21(0.03)	1.93(0.04)	0.071	BZB	A	0
2FGLJ2009.7+7225	J200952.29+722919.3	BZBJ2009+7229	1.07(0.03)	2.76(0.03)	2.41(0.06)	?	UND	B	1
2FGLJ2015.1-0137	J201515.15-013732.4	BZBJ2015-0137	0.96(0.03)	2.63(0.04)	2.16(0.08)	?	UND	C	1
2FGLJ2022.3-4518	J202226.40-451329.5	BZBJ2022-4513	0.95(0.04)	2.6(0.04)	2.14(0.07)	?	BZB	C	6
2FGLJ2022.5+7614	J202235.57+761126.1	BZBJ2022+7611	1.01(0.03)	2.82(0.03)	2.28(0.04)	?	UND	A	0
2FGLJ2023.4-1137	J202336.67-113957.5	BZQJ2023-1139	0.63(0.11)	3.71(0.19)	2.88(0.32)	0.698	-	-	-
2FGLJ2025.6-0736	J202540.65-073552.5	BZQJ2025-0735	1.19(0.04)	3.17(0.04)	2.56(0.07)	1.388	BZQ	B	0
2FGLJ2030.3-0622	J203015.14-062214.8	BZQJ2030-0622	1.22(0.04)	3.06(0.07)	1.72(0.32)	0.667	-	-	-
2FGLJ2031.7+1223	J203154.99+121941.5	BZBJ2031+1219	1.1(0.04)	3.05(0.06)	2.54(0.13)	1.215??	BZQ	C	0
2FGLJ2035.4+1058	J203522.28+105605.9	BZQJ2035+1056	0.66(0.03)	2.57(0.03)	2.37(0.08)	0.601	-	-	-
2FGLJ2039.1-1046	J203900.71-104641.7	BZBJ2039-1046	0.95(0.03)	2.57(0.03)	2.22(0.05)	?	UND	C	0
2FGLJ2050.0+0408	J205006.23+040749.0	BZBJ2050+0407	1.04(0.03)	2.79(0.04)	2.22(0.07)	?	UND	B	1
2FGLJ2055.4-0023	J205528.22-002117.0	BZBJ2055-0021	0.74(0.04)	2.29(0.1)	2.03(0.39)	?	-	-	-
2FGLJ2056.2-4715	J205616.35-471447.3	BZQJ2056-4714	1.27(0.03)	3.28(0.03)	2.52(0.04)	1.491	BZQ	A	0
2FGLJ2115.3+2932	J211529.41+293338.4	BZQJ2115+2933	1.17(0.04)	3.05(0.05)	2.37(0.11)	1.514	BZQ	C	0
2FGLJ2116.2+3339	J211614.52+333920.6	BZBJ2116+3339	0.73(0.03)	2.12(0.04)	1.9(0.08)	?	BZB	B	0
2FGLJ2121.0+1901	J212100.57+190128.4	BZQJ2121+1901	0.89(0.12)	2.35(0.45)	3.64(0.62)	2.18	-	-	-
2FGLJ2131.6-0914	J213135.41-091523.5	BZBJ2131-0915	0.71(0.04)	2.23(0.12)	2.45(0.33)	0.449	-	-	-
2FGLJ2133.8-0154	J213410.30-015317.1	BZBJ2134-0153	1.1(0.03)	2.92(0.03)	2.48(0.05)	1.283	BZQ	B	0
2FGLJ2139.3-4236	J213924.16-423520.3	BZBJ2139-4235	0.9(0.03)	2.48(0.03)	2.03(0.04)	?	BZB	A	0
2FGLJ2141.7-3739	J214152.44-372912.8	BZQJ2141-3729	1.1(0.04)	2.91(0.05)	2.7(0.08)	0.423	-	-	-
2FGLJ2143.2-3929	J214302.85-392924.7	BZBJ2143-3929	0.77(0.04)	2.22(0.11)	1.95(0.45)	?	-	-	-
2FGLJ2143.5+1743	J214335.55+174348.8	BZQJ2143+1743	1.09(0.03)	2.79(0.03)	2.43(0.03)	0.213	UND	C	0
2FGLJ2144.8-3356	J214501.13-335716.2	BZQJ2145-3357	1.11(0.04)	2.77(0.05)	2.44(0.13)	1.36	-	-	-
2FGLJ2146.5-1530	J214622.97-152543.6	BZQJ2146-1525	1.05(0.04)	2.96(0.05)	2.28(0.11)	0.698	UND	C	6
2FGLJ2147.3+0930	J214710.14+092946.4	BZQJ2147+0929	1.17(0.05)	2.84(0.1)	2.67(0.24)	1.113	BZQ	C	1
2FGLJ2147.4-7534	J214712.71-753613.0	BZQJ2147-7536	1.21(0.03)	3.12(0.02)	2.44(0.03)	1.138	BZQ	A	0
2FGLJ2148.2+0659	J214805.46+065738.7	BZQJ2148+0657	1.31(0.03)	2.7(0.03)	2.38(0.04)	0.999	-	-	-
2FGLJ2151.5-3021	J215155.51-302753.5	BZQJ2151-3027	1.05(0.04)	3.13(0.06)	2.09(0.1)	2.345	-	-	-
2FGLJ2152.4+1735	J215224.81+173437.8	BZBJ2152+1734	0.95(0.03)	2.59(0.03)	2.19(0.05)	?	UND	C	1
2FGLJ2154.0-1138	J215350.22-113613.9	BZQJ2153-1136	1.18(0.04)	3.0(0.05)	2.58(0.11)	1.582	BZQ	C	1
2FGLJ2157.4+3129	J215728.81+312701.4	BZQJ2157+3127	1.07(0.03)	2.9(0.03)	2.34(0.07)	1.488	UND	C	0
2FGLJ2157.9-1501	J215806.27-150109.0	BZQJ2158-1501	1.04(0.03)	2.79(0.03)	2.5(0.06)	0.672	UND	C	0
2FGLJ2158.8-3013	J215852.05-301332.0	BZBJ2158-3013	0.78(0.03)	2.13(0.03)	1.85(0.04)	0.116	BZB	A	0
2FGLJ2201.9-8335	J220219.20-833811.6	BZQJ2202-8338	1.09(0.03)	2.9(0.04)	2.33(0.1)	1.865	-	-	-
2FGLJ2202.8+4216	J220243.29+421640.0	BZBJ2202+4216	0.96(0.03)	2.53(0.03)	2.19(0.02)	0.069	UND	C	0
2FGLJ2203.4+1726	J220326.89+172548.3	BZQJ2203+1725	1.08(0.03)	2.84(0.03)	2.35(0.03)	1.076	UND	A	0
2FGLJ2206.6-0029	J220643.27-003102.3	BZBJ2206-0031	0.98(0.04)	2.71(0.04)	2.21(0.1)	?	UND	B	0
2FGLJ2208.1-5345	J220743.71-534633.6	BZQJ2207-5346	1.15(0.04)	2.92(0.05)	2.57(0.11)	1.215	BZQ	C	1
2FGLJ2211.9+2355	J221205.96+235540.7	BZQJ2212+2355	1.17(0.05)	2.73(0.12)	2.71(0.26)	1.125?	-	-	-
2FGLJ2213.1-2527	J221302.49-252929.9	BZQJ2213-2529	1.11(0.04)	3.02(0.04)	2.52(0.06)	1.833	BZQ	B	0
2FGLJ2217.1+2422	J221700.82+242146.0	BZBJ2217+2421	1.04(0.03)	2.79(0.03)	2.31(0.05)	0.505	UND	B	0
2FGLJ2219.1+1805	J221914.07+180635.8	BZQJ2219+1806	0.68(0.07)	3.17(0.14)	2.33(0.35)	1.802	-	-	-
2FGLJ2221.6-5223	J222129.30-522527.6	BZBJ2221-5225	0.72(0.03)	2.16(0.05)	1.94(0.17)	?	BZB	C	0
2FGLJ2222.0-3503	J222305.92-345547.0	BZQJ2223-3455	1.05(0.03)	2.93(0.03)	2.69(0.04)	0.298	-	-	-
2FGLJ2225.6-0454	J222547.25-045701.2	BZQJ2225-0457	1.19(0.03)	3.2(0.03)	2.53(0.04)	1.404	BZQ	B	0
2FGLJ2229.7-0832	J222940.08-083254.3	BZQJ2229-0832	1.14(0.03)	3.35(0.04)	2.6(0.05)	1.56	BZQ	B	0
2FGLJ2232.4+1143	J223236.40+114350.9	BZQJ2232+1143	1.28(0.03)	2.98(0.04)	2.39(0.07)	1.037	BZQ	B	0
2FGLJ2234.9-4831	J223513.23-483558.6	BZQJ2235-4835	1.11(0.03)	2.81(0.04)	2.46(0.07)	0.51	BZQ	C	3
2FGLJ2236.4+2828	J223622.47+282857.4	BZQJ2236+2828	1.02(0.03)	2.83(0.03)	2.36(0.03)	0.79	UND	A	0
2FGLJ2236.5-1431	J223634.08-143322.0	BZBJ2236-1433	1.08(0.03)	2.84(0.03)	2.34(0.04)	?	UND	A	0
2FGLJ2237.2-3920	J223708.10-392137.9	BZQJ2237-3921	0.96(0.03)	2.68(0.04)	2.29(0.11)	0.297	UND	B	0
2FGLJ2243.2-2540	J224326.40-254430.4	BZBJ2243-2544	1.04(0.03)	2.83(0.03)	2.3(0.06)	0.774	UND	B	0
2FGLJ2243.9+2021	J224354.74+202103.8	BZBJ2243+2021	0.85(0.03)	2.24(0.03)	1.96(0.07)	?	BZB	B	0
2FGLJ2244.1+4059	J224412.72+405713.7	BZBJ2244+4057	1.13(0.03)	2.94(0.04)	2.33(0.06)	?	BZQ	B	0
2FGLJ2247.2-0002	J224730.18+000006.7	BZBJ2247+0000	1.08(0.04)	2.86(0.08)	2.3(0.17)	?	UND	C	2
2FGLJ2250.0+3825	J225005.75+382437.3	BZBJ2250+3824	0.58(0.03)	1.86(0.04)	1.86(0.14)	0.119	BZB	B	0
2FGLJ2251.9+4032	J225159.77+403058.2	BZBJ2251+4030	0.79(0.03)	2.19(0.05)	1.81(0.11)	?	BZB	B	0
2FGLJ2253.9+1609	J225357.74+160853.6	BZQJ2253+1608	1.04(0.03)	2.92(0.02)	2.42(0.02)	0.859	UND	C	0
2FGLJ2255.2+2408	J225515.37+241011.4	BZBJ2255+2410	0.87(0.03)	2.25(0.04)	2.0(0.11)	?	BZB	B	0
2FGLJ2256.4-2009	J225641.19-201140.3	BZBJ2256-2011	1.06(0.03)	2.81(0.03)	2.32(0.06)	?	UND	B	0
2FGLJ2258.0-2759	J225805.95-275821.0	BZQJ2258-2758	1.16(0.03)	2.94(0.03)	2.46(0.03)	0.926	BZQ	A	0
2FGLJ2304.7+3703	J230436.71+370507.5	BZBJ2304+3705	0.65(0.04)	2.16(0.07)	2.05(0.26)	?	BZB	C	0
2FGLJ2308.0+1457	J230733.99+145018.1	BZBJ2307+1450	0.98(0.04)	2.76(0.05)	2.26(0.15)	0.503	-	-	-
2FGLJ2311.0+3425	J231105.32+342511.0	BZQJ2311+3425	1.1(0.03)	3.01(0.03)	2.4(0.05)	1.817	BZQ	B	0
2FGLJ2315.7-5014	J231544.32-501839.5	BZBJ2315-5018	1.09(0.03)	2.97(0.03)	2.45(0.05)	?	BZQ	B	0
2FGLJ2321.0+2737	J232159.86+273246.9	BZQJ2321+2732	0.93(0.04)	2.53(0.05)	2.34(0.15)	1.253	-	-	-
2FGLJ2322.2+3206	J232154.96+320407.7	BZQJ2321+3204	1.14(0.04)	2.9(0.05)	2.36(0.13)	1.489	BZQ	C	1
2FGLJ2322.6+3435	J232244.01+343613.9	BZBJ2322+3436	0.27(0.03)	1.62(0.07)	1.68(0.36)	0.098	-	-	-
2FGLJ2323.6-0316	J232331.94-031704.8	BZQJ2323-0317	1.14(0.03)	2.94(0.04)	2.36(0.07)	1.393	BZQ	B	0
2FGLJ2323.8+4212	J232352.07+421058.6	BZBJ2323+4210	0.75(0.03)	2.26(0.07)	1.45(0.42)	0.059?	-	-	-
2FGLJ2324.7-4042	J232444.65-404049.3	BZBJ2324-4040	0.74(0.03)	2.06(0.03)	1.62(0.1)	?	BZB	C	0
2FGLJ2325.3+3957	J232517.86+395736.5	BZBJ2325+3957	1.01(0.04)	2.63(0.06)	2.54(0.14)	?	UND	C	0
2FGLJ2325.4-4758	J232526.86-480017.0	BZBJ2325-4800	0.92(0.03)	2.43(0.03)	2.04(0.05)	0.221	BZB	A	0

*Continued on next page*

TABLE 8 – *Continued from previous page*

2FGL name	<i>WISE</i> name	ROMA-BZCAT name	[3.4]-[4.6] mag	[4.6]-[12] mag	[12]-[22] mag	z	type	class	$N_{BR}$
2FGLJ2327.5+0940	J232733.57+094009.8	BZQJ2327+0940	1.28(0.06)	3.24(0.09)	2.56(0.21)	1.843	BZQ	C	0
2FGLJ2329.2-4956	J232920.86-495540.5	BZQJ2329-4955	1.22(0.04)	3.19(0.03)	2.55(0.06)	0.518	BZQ	B	0
2FGLJ2330.6-3723	J233035.78-372437.8	BZBJ2330-3724	0.98(0.03)	2.84(0.03)	2.38(0.05)	0.279	UND	B	0
2FGLJ2330.9-2144	J233104.01-214815.0	BZQJ2331-2148	1.06(0.04)	2.8 (0.08)	2.25(0.21)	0.563	UND	C	0
2FGLJ2331.8-1607	J233138.63-155656.8	BZQJ2331-1556	1.07(0.05)	3.05(0.06)	2.51(0.16)	1.153	-	-	-
2FGLJ2334.3+0734	J233412.82+073627.6	BZQJ2334+0736	1.11(0.03)	2.82(0.04)	2.42(0.09)	0.401	-	-	-
2FGLJ2334.8+1431	J233453.82+143214.9	BZBJ2334+1432	0.9 (0.04)	2.4 (0.05)	2.03(0.18)	?	BZB	C	0
2FGLJ2336.3-4111	J233633.97-411521.7	BZQJ2336-4115	1.15(0.04)	3.01(0.06)	2.64(0.12)	1.406	BZQ	C	0
2FGLJ2338.1-0229	J233757.33-023057.4	BZQJ2337-0230	1.18(0.03)	3.01(0.03)	2.51(0.05)	1.071	BZQ	B	0
2FGLJ2339.0+2125	J233856.38+212441.3	BZBJ2338+2124	0.83(0.04)	2.36(0.05)	1.66(0.19)	0.291	-	-	-
2FGLJ2341.7+8016	J234054.23+801515.9	BZBJ2340+8015	0.71(0.03)	2.07(0.04)	1.76(0.11)	0.274	BZB	B	0
2FGLJ2345.0-1553	J234512.45-155507.7	BZQJ2345-1555	1.07(0.03)	2.81(0.03)	2.29(0.05)	0.621	UND	B	0
2FGLJ2347.9-1629	J234802.60-163111.9	BZQJ2348-1631	1.06(0.03)	2.78(0.03)	2.36(0.04)	0.576	UND	B	0
2FGLJ2353.5-3034	J235347.44-303748.2	BZBJ2353-3037	1.0 (0.04)	2.9 (0.04)	2.22(0.09)	?	UND	B	0
2FGLJ2359.0-3037	J235907.88-303740.5	BZBJ2359-3037	0.68(0.03)	2.05(0.06)	1.68(0.27)	0.165	BZB	C	0

